ENN Encyclopedia of Nanoscience and Nanotechnology
www.aspbs.com/enn

Functionalities of Dendrimers

Toyoko Imae

Nagoya University, Nagoya, Japan

Katsuya Funayama, Yuko Nakanishi, Kenkichi Yoshii

Nagoya University, Nagoya, Japan

CONTENTS

1. INTRODUCTION

The structures and properties of novel dendritic polymers—dendrimers—have been studied extensively as nanomolecules with the attractive, potential applications in a variety of fields [1–8]. In particular, the investigations are focused on the phenomena based on the concept of "dendritic boxes" or "unimolecular micelles" for the capture of guest molecules and as the compartment of chemical reaction. Host-guest systems, consisting of dendrimers, have enormous demands in the fields of molecular recognition and transport, such as drug delivery, gene therapy, and chemical separation.The interest in dendritic polymers for such applications stems from their distinctive dual structural properties, an external periphery bearing multiple functional groups for solubilization in media and an internal region possessing cavities for the capsulation of small molecules.

Novel dendrimers are prepared by covalent bonding from a functional core through the successive repeating synthesis of a spacer and a branching part (divergent method) or from a conjugation at the conic center of dendrons, units of a dendrimer, (convergent method). When two steps are needed for the extension of repeating units, each step is called a half generation. While the structures of dendrimers at low generations are opened and asymmetric, the structures become crowded and spherical during the increase of the generation [9]. These structural changes influence the properties of dendrimers. Then, dendrimers have a unique surface of plural terminal groups, the number of which can be accurately controlled on a synthesis process. Furthermore, it is possible to bind covalently different functional units in the core, branches, and terminal groups on the divergent synthesis process and to conjugate the dendrons of different chemical constituents on the convergent synthesis process. Thus, dendrimers having various structures and properties can be synthesized.

In this article, the up-to-date investigations concerning the functionalities of dendrimers are reviewed. In particular, dendrimer properties of doping, molecular recognition, adsorption, and hybridization are the focus, and the phenomena of solubilization, complexiation, self-organization, and nanocomposite formation are discussed in relation to the structures and functionalities of dendrimers.

2. DOPING AND SOLUBILIZATION OF GUEST MOLECULES

It is well established that the solubility of hydrophobic molecules in water can be dramatically enhanced in the presence of water-soluble, surface-active agents. For instance, the number of pyrene molecules solubilized in nonionic surfactant micelles of heptaethyleneoxide monoalkyl ether (C_nE_7) has been found to be linearly proportional to the aggregation number of the micelles [10]. The solubilization capacity for pyrene is low in spherical micelles of ionic dodecyl sulfate, limited at most to two pyrenes per micelle [11]. Since dendrimers have cavity for maintaining small molecules and may be regarded as unimolecular micelles, water-soluble dendrimers are expected to

ISBN: 1-58883-059-4/$35.00

Encyclopedia of Nanoscience and Nanotechnology
Edited by H. S. Nalwa
Volume 3: Pages (685–701)

increase the solubility of water-insoluble or weakly soluble organic compounds. The solubilization of guest molecules in such dendrimers has been investigated mostly by a fluorescence probing agent—pyrene [9, 12–15]. Caminanti et al. [9] have used pyrene as a photoluminescence probe to sense hydrophobic sites in poly(amido amine) (PAMAM) dendrimers possessing sodium carboxylated surfaces. The probe method provided experimental evidence for a surface structural transition between generations 3.5 to 4.5. Pistolis et al. [12, 13] have reported that the solubilizing capability of amine-terminated PAMAM and amine-terminated poly(propylene imine) (PPI) dendrimers in aqueous media increases with increasing their generations. Pyrene fluorescence undergoes significant quenching in the solubilized state, and excimer fluorescence is observed. It has been also concluded, by the findings concerning exciplex formation, that water is progressively excluded from the dendrimer interior, as the generation of PPI dendrimer increases. It has been reported by Schmitzer et al. [14] that glucose-persubstituted PAMAM dendrimers increase solubilizate quantities of pyrene and benzoylcyclohexane in water, depending on the number of microcavities in each dendrimer, although the solubility of pyrene is 3–4 times larger than that of benzoylcyclohexane. Quaternary ammonium chloride PPI dendrimers with both hydrophilic (triethylenoxy methyl ether) and hydrophobic (octyl) chain ends have been synthesized by Pan and Ford [15]. These amphiphilic dendrimers solubilize pyrene in aqueous solution, and the limiting solubility corresponds to one pyrene per dendrimer molecule.

In order to clarify the solubilization capacity of dendrimers, depending on structures and conditions, we have investigated ultraviolet-visible and steady-state fluorescence spectroscopy of aromatic guest molecules in aqueous solutions of fourth generation PAMAM dendrimer with hydroxyl and amine terminals (G4 PAMAM-OH dendrimer, G4 PAMAM-NH_2 dendrimer) and fourth and fifth generation PPI dendrimers with amine terminals (G4 and G5 PPI-NH_2 dendrimers) as host molecules. As seen in Figures 1 and 2, pyrene is soluble in aqueous solutions of dendrimers, although the solubility of pyrene in dendrimers depends on terminal groups, internal chemical structures, and generations of dendrimers as well as pH. On the other hand, a guest molecule larger than pyrene—benzopyrene—is not solubilized because of its larger size. However, the solubility of phenantherene and benzene are also not enhanced in the presence of dendrimers under the same conditions, except the solubility (0.2) of phenanthrene into an aqueous solution of G4 PAMAM-NH_2 dendrimer at pH 11.01. Phenanthrene and benzene are presumably too small, in comparison to the sizes of microcavities in dendrimers studied, and easily pass through the cavities. Therefore, the structural matching of guest molecules noninteracting with dendrimers plays an important role in their doping into the microcavities of dendrimers.

Since dendrimers with tertiary amine groups in interior and primary amine groups in exterior have pKa of 6.65 and 9.20, respectively, the electric charges of dendrimers change with the pH of the aqueous solutions of dendrimers [16]. The solubility of pyrene in aqueous solutions of dendrimers below pH 6.65 is larger than above

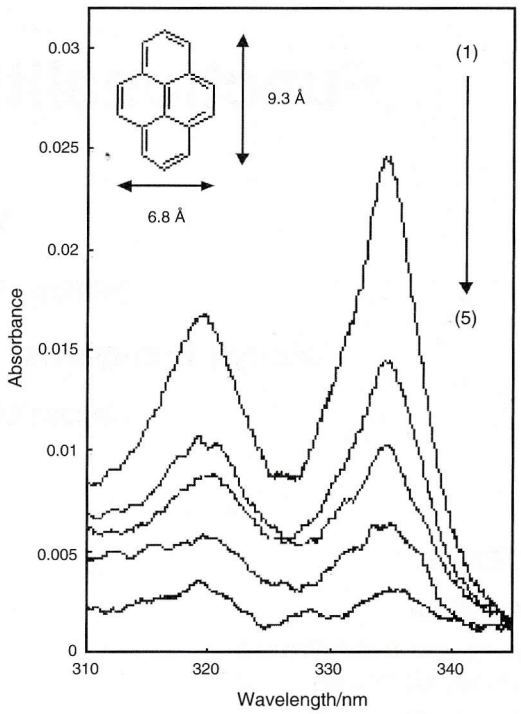

Figure 1. UV-visible spectra of pyrene solubilized in aqueous solutions with and without dendrimers at 25 °C. Powder of guest molecules was added into aqueous solutions of dendrimers at a concentration of 5.0×10^{-7} M, which were adjusted at pH ~6. After the mixtures were stirred overnight, excess guest molecules insoluble in the solutions of dendrimers were filtrated out. Then, UV-visible spectra of the filtrates were measured. From top to bottom: (1) fourth generation hydroxyl-terminated PAMAM dendrimer at pH 5.85; (2) fifth generation amine-terminated PPI dendrimer at pH 6.01; (3) fourth generation amine-terminated PAMAM dendrimer at pH 5.99; (4) fourth generation amine-terminated PPI dendrimer at pH 5.91; (5) without dendrimer.

pH 6.65 (see Fig. 2). This indicates that the protonation of amine groups in interior influences in the doping of pyrene, since the microcavities in the dendrimers are expanded into the preferable sizes by the protonation. Chen et al. [17] have caught the clear evidence for a pH-responsive conformational change of PAMAM dendrimer with amine terminals by means of polarity changes of a polarity-responsive probe, although they could not distinguish between the "denser shell" and "denser core" models. The solubility of pyrene in G4 PAMAM-OH dendrimer is higher than that in G4 PAMAM-NH_2 dendrimer (see Fig. 2). Dendrimers with protonated hydrophilic terminal groups may exclude hydrophobic organic molecules to approach, in contrast to dendrimers with nonionic terminal groups. Incidentally, a positively charged G4 PAMAM-NH_2 dendrimer has demonstrated having "closed" structure [18]. The dimensions of the charged dendrimers have been investigated for carboxylic acid-functionalized PPI dendrimers [19]. The dimension is larger for charged dendrimers and the uncharged dendrimers have the lowest radius. Therefore, the size change of dendrimers occurs with pH.

One must notice that the size change of dendrimers depends not only on the functionality of the branching

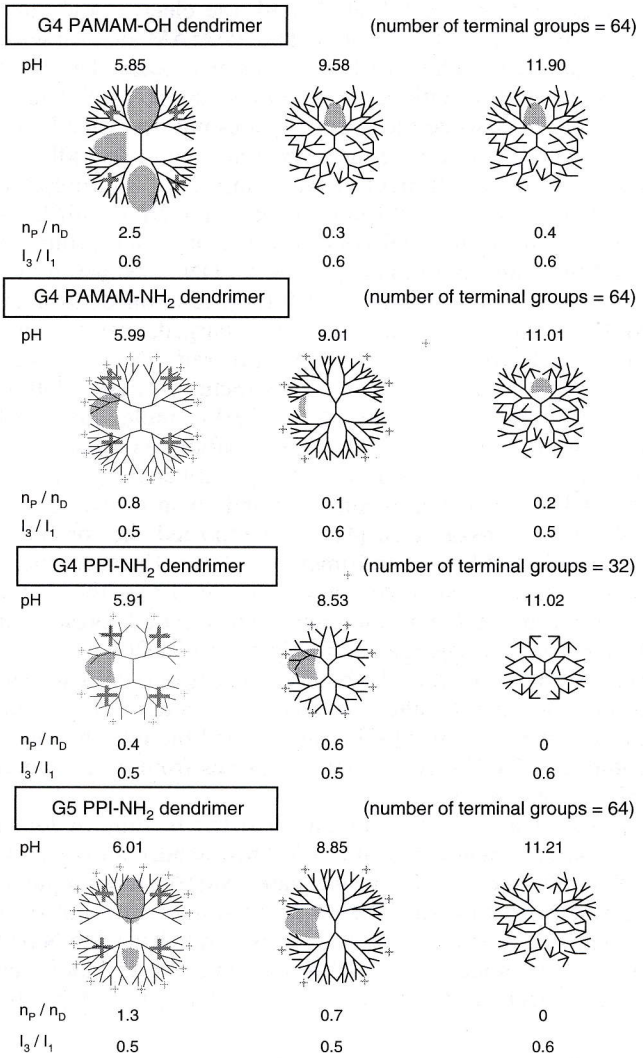

Figure 2. Solubility of pyrene in aqueous solutions of dendrimers at different pHs at 25 °C. The molar fractions of guest molecules per dendrimer were calculated by using molar extinction coefficients of guest molecules (1.7×10^7 cm^2mole^{-1} at 337 nm for pyrene, 1.4×10^7 cm^2mole^{-1} at 293 nm for phenanthrene). n_P/n_D = number of pyrene molecules solubilized in a dendrimer (solubility). I_3/I_1 = ratio of the third (I_3, 386 nm) to the first (I_1, 375 nm) monomer fluorescence emission intensities of pyrene (polarity index).

points and the functional terminal groups but also on the core, size of spacer, and generation. Although G5 PPI-NH_2 dendrimer and G4 PAMAM-NH_2 dendrimer have the same number and property of terminal groups, the solubility of pyrene in solutions of G5 PPI-NH_2 dendrimer is higher than that of G4 PAMAM-NH_2 dendrimer (see Fig. 2). Since the segment density of a PPI dendrimer is lower than that of a PAMAM dendrimer, due to a longer core alkyl chain [20], guest molecules are doped easier in a PPI dendrimer. The solubility is superior in solutions of G5 PPI-NH_2 dendrimer than in solutions of G4 homologue (see Fig. 2), because of larger volume or microcavity, as found in the solubilization of pyrene in CnE_7 micelles [10].

Pyrene is a useful fluorescence probe for getting micropolarity around it. Micropolarities around solubilization sites of dendrimers can be evaluated as the ratio of the third to the first monomeric fluorescence emission intensities of pyrene, which is well known as a polarity index. As seen in Figure 2, the polarity index of pyrene in aqueous solutions of all dendrimers is close to that in water and independent of the pH. It can be predicted that pyrene exists in the hydrophilic environment in dendrimers, which is invented by the penetration of water [20]. This causes the less solubility of pyrene in dendrimers than in the hydrophobic interior in surfactant micelles, where a larger amount of pyrene is solubilized [10]. Caminati et al. [9] have revealed that pyrene is probably bound in the hydrophilic palisade layer of the PAMAM dendrimer at the small distance from the charged surface groups, supporting the conclusion previously described.

Besides determining the solubilization capacity of dendrimers, extensive works have been reported on the behaviors of solubilized pyrene in dendrimer assemblies and of covalent-bonded pyrene in dendrimers [21–23]. The solubilization of pyrene was used for the determination of micellar formation of amphiphilic linear-dendritic diblock copolymers consisting of hydrophilic linear polyethylene oxide and hydrophobic dendritic carbosilane [21]: The critical micelle concentrations were determined from pyrene fluorescence. It was also found that increasing the size of dendritic block increases the partition equilibrium constants of pyrene in micellar solution. The steady-state fluorescence anisotropy of 1,6-diphenyl-1,3,5-hexatriene in micelles of amphiphilic linear-dendritic diblock copolymers are lower than that of the linear polymeric amphiphiles, suggesting that the microviscosity of the dendritic micellar core is lower than those of linear polymeric micelles. Baker and Crooks [22] have synthesized four generations of PPI dendrimers, which are covalently modified with pyrene moieties, and compared the behavior of pyrene moieties with those of pyrene solubilized in dendrimers. More intensive excimer emission was observed for higher generation dendrimers, while little or no evidence for interdendrimer interactions was observed. Protonation of the tertiary amine units increased monomer fluorescence significantly, while there was only a slight increase in the observed excimer fluorescence. The excitation energy transfer has been investigated between a first generation dendrimer as a donor molecule and a pyrene-containing polymer as an acceptor molecule in Langmuir–Blodgett monolayers [23]. The adjacent donor and accepter layers dramatically increased the fluorescence activity of the pyrene group in a pyrene-containing polymer.

3. MOLECULAR RECOGNITION AND COMPLEXIATION WITH LINEAR POLYMERS

Dendrimers are regularly branched polymers possessing a large number of surface functional groups [24–30]. Their molecular recognition ability is strongly influenced by the nature of the terminal functionalities. The number of terminal groups of dendrimers is increased by the number of branching sites with increasing their generation. Since the terminals behave as functional groups, dendrimers are useful as probes of molecular recognition and carriers

of molecular transport. Dendrimers with ionic terminal groups electrostatically interact with counter-ionic groups. Such interaction is useful for catching linear polymers on interpolyelectrolyte complexiation. Many researches for such complexiation were carried out for native polymers [31–43] and synthetic polymers [44–49].

The investigations of the complexation with DNA were performed from the view of gene delivery in mammalian organisms. Since dendrimers are spherical molecules with a size comparable to histone, which is a gene-transporting globular protein, the biomimetic investigation for DNA transfer in the living cells was carried out by using PAMAM dendrimers [31–36]. Plank et al. [31] have examined the complement-activating properties of synthetic cationic molecules and their complexes with DNA. While strong complement activation was seen with a fifth generation PAMAM dendrimer, on the complexiation with DNA it depended on the ratio of polycation and DNA. The ability of PAMAM dendrimers to bind DNAs in a variety of mammalian cells and to enhance their transfer has been investigated by Kukowska-Latallo et al. [32, 33]. Since dendrimers bind various forms of nucleic acids on the basis of electrostatic interaction, the ability of DNA-dendrimer complexes for transfering oligonucleotides and plasmid DNA to mediate antisense inhibition was assessed in an *in-vitro* cell culture system. Although the capability of dendrimers to transfect cells appears to depend on the size and shape of dendrimers and the number of primary amine groups on the surface of the dendrimers, the results indicate that dendrimers function as an effective delivery system. Tang et al. [34] have reported that the transfection activity of the dendrimers is dramatically enhanced by heat treatment. The increased transfection after the heating process is principally due to the increase in flexibility which enables the dendrimer to be compact at the complexiation with DNA and swell at the release from DNA. Gebhart and Kabanov [35] have evaluated nonviral transfection *in vitro*, based on the complexes of DNA and polycations, with respect to their effectiveness, toxicity, and cell-type dependence. The effects of PAMAM and PPI dendrimers were compared to those of other polycations. Luo et al. [36] have chemically modified fifth generation PAMAM dendrimer with biocompatible poly(ethylene glycol) (PEG) chains. This novel conjugate produced a 20-fold increase in transfection efficiency in comparison with partly degraded dendrimer controls. Since the cytotoxicity of PEGylated dendrimer is very low, this kind of compound should be extremely efficient, highly biocompatible, and a low-cost DNA delivery system.

The physicochemical properties, interactions, and structures of DNA-dendrimer complexes have been investigated apart from the gene transport [37–42]. It has been proved by Ottaviani et al. [37] that the concentration dependence of the interaction between polynucleotide and dendrimers is different between small (second generation) and large (sixth generation) dendrimers. The interaction with small dendrimers decreased with an increase in concentration due to self-aggregation of dendrimer molecules. Conversely, the interaction with large dendrimers increased until saturation of the interacting sites occurred. It has also been demonstrated that the supramolecular structure of the complexes changes by varying the mixing ratio of DNA and dendrimers [38]. According to Chen et al. [39], the electrostatic interaction between polynucleotide and PAMAM dendrimer is essential for the effective DNA transfer process. The DNA wraps around seventh generation dendrimers, as illustrated in Figure 3(a), while the wrapping does not occur for fourth and lower generation dendrimers. Kabanov et al. [40] have clarified that electroneutral water-insoluble interpolyelectrolyte complexes of PPI dendrimers interacting with DNA are formed at an equal concentration of amine groups of dendrimer and phosphate groups of DNA. However, the excess addition of fourth- and fifth-generation dendrimers to DNA solution forms positively charged, water-soluble interpolyelectrolyte complexes. Complexed DNA compacts, revealing a wound double-helical structure. These relations may be compared with the Monte Carlo simulations, which were used in the study of the complexation between a polyelectrolyte and an oppositely charged spherical particle in the Debye–Hückel approximation and chain rigidity effects [50, 51]. Bielinska et al. [41] have reported the formation of complicated DNA-dendrimer complexes. Electron microscopic examination of complexes indicated that the majority of plasmid DNA is contracted into isolated toroids, but larger irregular aggregates of polymer and DNA also coexist. This indicates that the binding of plasmid DNA to dendrimer appears to alter its secondary and tertiary structures. Mitra and Imae [42] have revealed the morphology of complicated DNA-dendrimer complexes from atomic force microscopic observation.

Imae et al. [43] have investigated the binding of fourth generation amine-terminated PAMAM dendrimer on native polysaccharide, sodium hyaluronate (NaHA), in an aqueous 0.25 M NaCl solution. The observed variation of molecular weight as a function of mixing ratios of dendrimer to NaHA obeyed the model, where an average number of dendrimers binds to each NaHA chain. However, at a high mixing ratio,

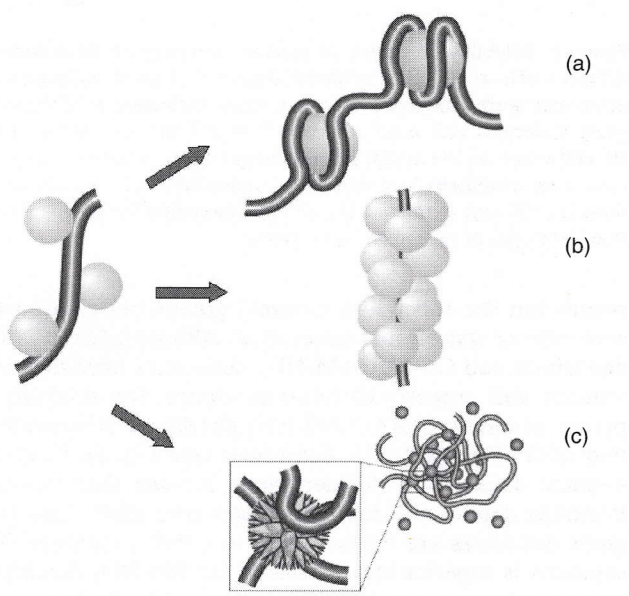

Figure 3. Binding models of cationic dendrimers on linear anionic polymers in solutions: (a) dendrimer-DNA complex; (b) dendrimer-sodium hyaluronate complex; (c) dendrimer-sodium poly(L-glutamate) complex.

the binding is saturated at two dendrimers per three repeating units on a NaHA chain, as illustrated in Figure 3(b). Whereas, at the initial stage of the addition of dendrimer, in a solution, NaHA maintains a worm-like character similar to NaHA without bound dendrimers, NaHA behave like a rigid rod at high dendrimer concentrations. In the NaHA-dendrimer complexiation, the hydrogen-bonding interaction, besides the electrostatic interaction, should play an important role.

The investigation has also been performed for the binding of dendrimers to synthetic linear polyelectrolytes with pH-dependent charge density [44–48]. Dubin et al. [44–47] have reported the complexiation between polycations and carboxylated dendrimers. The complexiation with poly(diallyldimethylammonium chloride) and other polycations occurs most readily for the 7.5th generation with high-charge density and does abruptly at a critical pH. The proposed model is that the polyelectrolyte backbone in the complex is distorted for bending around the contour of the spherical macroions [46]. The interaction of PPI dendrimers to a linear polyanion was compared with that to DNA by Kabanov et al. [48]. That is, dendrimers are penetrable for flexible oppositely charged polyelectrolyte chains. However, rigid negatively charged DNA double helixes apparently bind only to the dendrimer shell. The mixtures of dendrimers with polyanions containing equal amounts of cationic and anionic groups consist of mostly water-insoluble, ion-pair (stoichiometric) complexes but include water-soluble nonstoichiometric interpolyelectrolyte complexes.

The binding of PAMAM dendrimers on sodium poly-L-glutamates (NaPGA) in an aqueous 0.25 M NaCl solution has been reported by Imae and Miura [49]. The apparent molecular weight and the radius of gyration increased rapidly above a certain mixing ratio of dendrimer to NaPGA. The numerical analysis supported the aggregation model that free dendrimers are in equilibrium with dendrimers bound to NaPGA. Dendrimer-NaPGA complexes make aggregates in solution through the junction of dendrimer, and the aggregates consist of i-mer of dendrimer-NaPGA complexes, as shown in Figure 3(c). The aggregates take globular structure with a larger size than that of a single NaPGA without bound dendrimers.

The interesting aspect is the different complexiations of dendrimers with different linear polyelectrolytes such as DNA, NaHA, and NaPGA chains. They depend on the chemical and morphological structures of linear polyelectrolytes. The persistence lengths of the polyelectrolyte chains decrease in the order of rather rigid DNA > semi-flexible NaHA > randomly coiled NaPGA. The common is the electrostatic interaction of charged dendrimers with oppositely charged polyelectrolytes. Additionally, amide or hydroxyl groups in hyaluronate make hydrogen bonding with amide groups in PAMAM dendrimer, and, as a result, many dendrimers are attracted on a NaHA chain, where the steric and electrostatic repulsions between bound guest polyelectrolytes stretch the host polyelectrolyte chain. On the other hand, dendrimers act as a junction connecting between NaPGA chains, and the dendrimer-NaPGA complexes change from "intramolecular" (several guest polyelectrolytes attached to a single host polyelectrolyte) to "intermolecular" (containing more than one host polyelectrolyte), as found in mixtures of polyelectrolytes and surfactant micelles [52]. In the case of DNA, the morphology of complexes with dendrimers is complicated. It seems that the aggregation of complexes occurs simultaneously with the isolated DNA toroid formation including dendrimers and the aggregate sizes are not controlled.

Welch and Muthukumar [53] have examined by the computer simulation based on the theoretical background, the equilibrium and dynamic complexiation behavior of monocentric dendrimer with charged terminal groups to a flexible, oppositely charged polyelectrolyte. They noted three different types of complexes depending upon the ionic strength of solution, the size of the dendrimer, and the length of polymer chain. In three complexes, a dendrimer encapsulates a flexible polyelectrolyte chain, mutually interpenetrates with it, or walks along it. Chodanowski and Stoll [50, 51] have also proposed, as computer-simulated results, the pictures of aggregates of charged dendrimers with oppositely charged polyelectrolytes and the conditions necessary for forming aggregates, such as chain rigidity. Three types of complexes depend upon the ionic strength of solution and the size of the dendrimer or polymer chain, being similar to the results by Welch and Muthukumar [53]. However, both groups did not attach importance to the aggregation of complexes.

We have focused on "intermolecular" dendrimer-NaPGA complexiation. The small-angle X-ray scattering (SAXS) intensity $I(Q)$ at a scattering vector Q for particle solutions is contributed by the number of density particles, the intraparticle form factor depending on the particle geometry, and the interparticle structure factor that is related to the interparticle interactions [20, 54–57]. Figure 4(a) shows SAXS profiles of aqueous 0.25 M NaCl solutions of fourth generation amine-terminated PAMAM dendrimer and its mixture with NaPGA. There is the difference between two $I(Q)$ curves, and both have a peak at $Q = 0.055$ or 0.07 A^{-1}. Moreover, SAXS intensities of PAMAM dendrimer decreased with the addition of NaPGA, indicating the interaction between dendrimers and NaPGAs. The complexiation and the aggregation between dendrimer and NaPGA were also supported from dynamic light scattering. Main hydrodynamic diameter (149.4 nm) for a solution of dendrimer-NaPGA mixture was larger than those of free dendrimer (6.2 nm) and free NaPGA.

Normalized intermediate correlation function $I(Q, t)/I(Q, 0)$ at a time t from neutron spin echo (NSE) for particle dynamics, which is contributed by two diffusion modes, is described by a double-decaying exponential function [57–60]. As seen in Figure 4(b), the experimental data for a 0.25 M NaCl solution of fourth generation amine-terminated PAMAM dendrimer-NaPGA complex is described by a double-decaying exponential function, although the contribution of the fast mode is small (3–9%) the same as in a case of free dendrimer [60]. This mode may originate in the deformation motion of dendrimer [57]. The major effective diffusion coefficient, that is, the coefficient of the slow mode ($6\sim8 \times 10^{-11}$ m^2s^{-1}), is comparable to the hydrodynamic translational diffusion coefficient ($2\sim3 \times 10^{-11}$ m^2s^{-1}) of the complex obtained from dynamic light scattering. This indicates the translational motion of dendrimers is not disturbed by the complexiation.

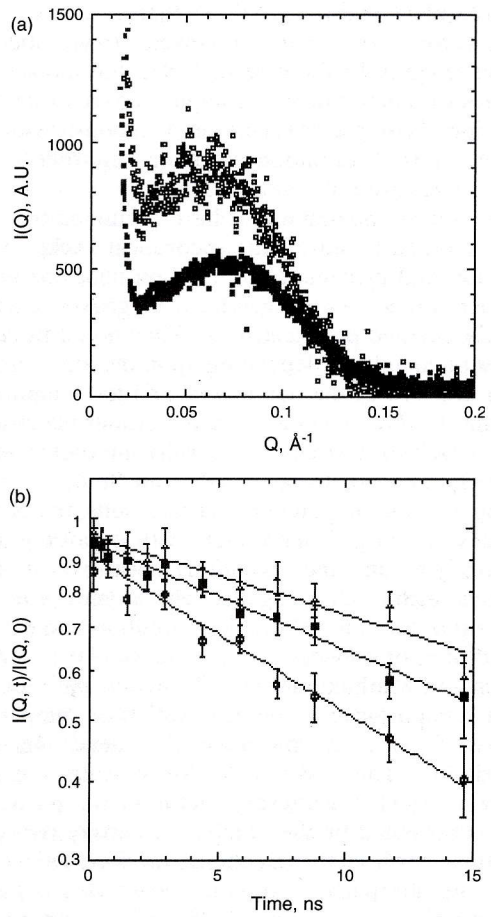

Figure 4. (a) Small-angle X-ray scattering intensities $I(Q)$ as a function of scattering vector Q for aqueous 0.25 M NaCl solutions of fourth generation amine-terminated PAMAM dendrimer (□) and fourth generation amine-terminated PAMAM dendrimer-sodium poly(L-glutamate) mixture (■). Dendrimer and poly(L-glutamate) concentrations are 5 and 0.1 wt%, respectively, and then a number ratio of amine terminal groups of dendrimer against side chains of sodium poly(L-glutamate) is 34.6. (b) Normalized intermediate scattering functions $I(Q, t)/I(Q, 0)$ as a function of time t for a 0.25 M NaCl solution of fourth generation amine-terminated PAMAM dendrimer-sodium poly(L-glutamate) mixture. Q (Å^{-1}); △, 0.06: ■, 0.08: ○, 0.1. Solid lines are theoretical ones with a decaying exponential function.

Interpolyelectrolyte complex formation between fourth generation amine-terminated PAMAM dendrimer and NaPGA in aqueous 0.25 M NaCl solution has been studied as a function of pH by Leisner and Imae [61]. Coacervation was observed at pH ~9 and it increased slightly with the dendrimer excess. Three relaxation modes were revealed from dynamic light scattering. The relaxation times of the faster modes are attributed to the hydrodynamic translational diffusions of dendrimer and of the interpolyelectrolyte complex. An additional slow mode dominates the multiexponential dynamic structure factor of the solution of interpolyelectrolyte complex network or the micro-gel inhomogeneity fluctuation. This mode is also associated with a sharp increase of the radius of gyration of mesoscopic particles from ~50 to ~250 nm.

4. ADSORPTION AND SELF-ORGANIZATION AT INTERFACES

4.1. Two-Dimensional Array in Bulk

One of novel utilizations of dendrimers is the construction of self-assemblies and supramolecular assemblies as building blocks, being valuable for the fabrication of higher ordered architectures. The structures of dendritic groups were discussed in relation to their self-assemblies and the liquid crystal formation was predicted [62]. Persec et al. [63, 64] have reported thermotropic nematic liquid crystal formation by dendritic polyethers. Poly(phenylenevinylene)s substituted with dendritic side chains also yielded thermotropic nematic liquid crystals [65]. Hudson et al. [66, 67] have found that flat, tapered, and conical monodendrons, respectively, self-assemble in hexagonal columnar and cubic thermotropic liquid crystal phases with high uniformity. The functionalization of poly(propylene imine) dendrimers with cholesteryl moieties through a carbamate linkage resulted in the formation of smectic A phases at a broad thermal range [68]. A series of polynorbornenes containing second-generation monodendrons as side chain have been synthesized [69]. Although the mesogens are rodlike, the polymers are conformationally flexible overall and displayed liquid-crystal behavior—during cooling, a nematic, smectic, and hexatic phase were observed.

In the cases described above, dendritic polymers with unique structures form the liquid crystals. Now it is assumed that the formation of anisotropically ordered architecture of dendrimers without unique structures is possible, once templates like liquid crystals are used. The lamellar liquid crystal of the cationic surfactant, didodecyldimethylammonium bromide (DDAB) in water, was selected as a template of two-dimensional architecture of anionic PAMAM dendrimers possessing carboxylate terminal groups [70]. The incorporation of dendrimers into the lamellar liquid crystal, at DDAB concentrations in the range of 4–30 wt %, resulted in the transition from a monophasic lamellar structure (L_α) to biphasic lamellar mixtures (L_α and L_α^D), at a similar molar mixing ratio for two dendrimers of 2.5 and 4.5 generations, as illustrated in Figure 5. The anionic dendrimer molecules doped into the water domains stick to the DDAB bilayers in the L_α structure, due to the stronger electrostatic interaction between the cationic surfactants and the oppositely charged dendrimers. In the narrow-spaced L_α^D structure, monolayers of flattened dendrimers are adsorbed between the DDAB bilayers, since the thicknesses of the dendrimer monolayers are smaller than the diameters of the corresponding dendrimers in aqueous solutions.

The investigations on the binding interactions and aggregation processes between dendrimers and surfactants have been carried out at low surfactant concentrations. Those are concerned with the supramolecular assemblies of surfactants with dendrimers [71–74], the dendrimer adsorption onto micelle surface [75, 76], and the structural modification of vesicles upon the interaction with dendrimers [77, 78]. The supramolecular assemblies are constructed by the primary noncooperative binding of monomeric surfactants and the secondary cooperative binding of micelle-like surfactants

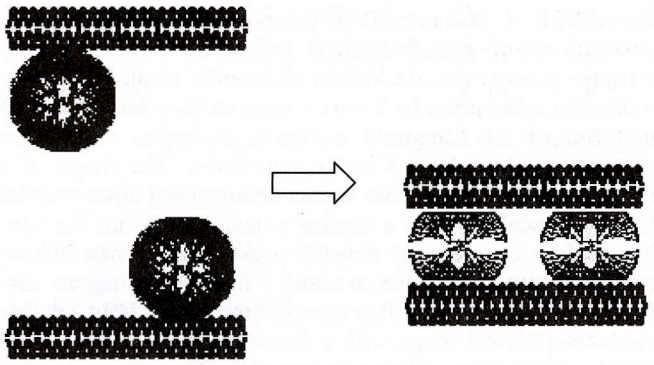

Figure 5. Schematic models of the lamellar L_α structure (left) and the lamellar L_α^D structure (right) in mixtures of didodecyldimethylammonium bromide, anionic PAMAM dendrimer, and water. Reprinted with permission from [70], X. Li et al., *J. Phys. Chem. B* 106, 12170 (2002). © 2002, American Chemical Society.

in/on dendrimer [71, 73]. Conversely, the reports at high surfactant concentrations are very few [79, 80]. Friberg et al. [79] have reported the formation of lamellar liquid crystal by octanoic acid and poly(ethylene imine) dendrimer. A third-generation dendrimer served as a solvent in the liquid crystal, and surfactants ionized and formed ionic pairs with amine terminals of dendrimer. Baars et al. [80] have investigated the scattering on the addition of dendrimers to continuous liquid crystals, but did not refer the morphology of hybrid liquid crystal structures.

4.2. Adlayers

Organization of dendrimers can be attained by the construction of one-, two-, and three-dimensional architectures. Especially, two-dimensional ordering is readily formed at air-liquid, air-solid, solid-liquid, and liquid-liquid interfaces. It is well known that traditional low-molecular-weight surfactants consist of hydrophilic head and lipophilic tail moieties and are characterized as typical amphiphilic molecules owing to their surface activity and association behavior. These kinds of molecules are suitable materials for the organization at the interface. On the process of the stepwise synthesis of dendrimers, central core, spacer, branch, and terminal group can be modified, and a variety of functional moieties or blocks are conjugated in dendrimers. Then, amphiphilic (hydrophilic and hydrophobic) characters can be introduced in dendrimers [81].

Linear polymer-dendrimer hybrids with unique head-tail structure have been synthesized [82–91]. Such copolymers with novel chemical structure possess specific characteristics such as amphiphilicity besides intrinsic dendritic and polymeric characters. They are surface active and arranged as a monolayer at the air-water interface. Amphiphilic dendrimers with a spherical shape have also been synthesized. Core-shell block dendrimers have different amphiphilicity at interior concentric generation layers and exterior generation layers [92–96]. Surface-block dendrimers have a character that the amphiphilicity of two hemispherical parts in dendrimers is different [82, 97–102]. That is, amphiphilic surface-block dendrimers consist of surface blocks with different affinities for solvents, where one is hydrophilic and the other is hydrophobic. Such structural character is dominant not only to associate into micelles, vesicles, microemulsions, liquid crystals, and other self-assemblies but also to adsorb at interfaces. Recently, Imae [81] has reviewed the association behavior of amphiphilic dendritic polymers.

Two dimensionally organized systems of amphiphilic dendrimers are prepared as Langmuir or Gibbs monolayer at an air-water interface and adsorption layer or self-assembled monolayer on solid substrate. Gibbs monolayer formation of amphiphilic dendrimers has been investigated for third and fourth generation amphiphilic surface-block dendrimers with amine and n-hexyl terminals (amine/hexyl), hydroxyl and n-hexyl terminals (hydroxyl/hexyl) and N-acetyl-D-glucosamine and n-hexyl terminals (glucosamine/hexyl) at the air-water interface [81, 99]. The organized adlayer formation and adsorption kinetics have been reported for the same dendrimers on the liquid-solid interfaces [101, 102]. The amine/hexyl and hydroxyl/hexyl dendrimers formed bilayers and their accumulation, owing to their amphiphilic character, which were different from the disordered adsorption of symmetric PAMAM dendrimer, as seen in Figure 6. Dendrimers in the bilayer form the flattened "pancake" structure by pairing between hydrophobic surface blocks. The hydrophilic terminals face to the solution and the solid substrate, since the adsorption film surface is hydrophilic. On the other hand, the adlayer of the glucosamine/hexyl dendrimers was rather flat. The time dependence of the adlayer formation was monitored *in-situ*. It proceeded through fast and slow adsorption steps. The adsorbed amount at the equilibrium decreased in the order of hydroxyl/hexyl > amine/hexyl > glucosamine/hexyl dendrimers and increased linearly with dendrimer concentration. The adsorption was abundant for the third

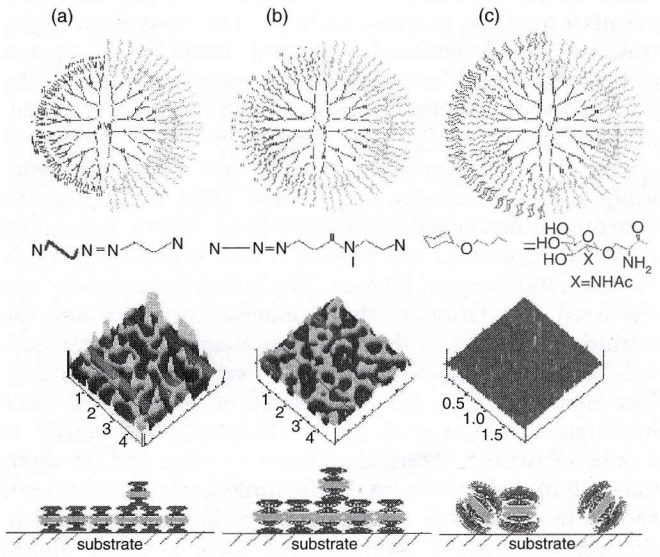

Figure 6. Adlayer formation by amphiphilic surface-block dendrimers on solid substrates. Reprinted with permission from [102], M. Ito et al., *Langmuir* 18, 9757 (2002). © 2002, American Chemical Society. (Top) chemical structure; (middle) atomic force microscopic image; (bottom) Adlayer model. (a) Fourth generation amine/hexyl PAMAM dendrimer; (b) fourth generation hydroxyl/hexyl PAMAM dendrimer; (c) fourth generation glucosamine/hexyl PAMAM dendrimer.

generation dendrimer in comparison to the fourth generation dendrimer and proceeded more for surface-block dendrimers than for PAMAM dendrimer in relation to the hydrophilicity-hydrophobicity balance of dendrimers. The molecular orientation of the hexyl chains in the adlayers was in the order of amine/hexyl > hydroxyl/hexyl > glucosamine/hexyl dendrimers.

Functional dendrimers of symmetrically branched structure are also focused as building blocks of the architectures such as thin adlayer films on solid substrates. Watanabe and Regen [103] have reported multilayer construction by PAMAM dendrimers on solid substrate. Adsorption and aggregation of carbosilane dendrimers and their hydroxyl- or mesogen substitutes on mica and pyrolytic graphite have been investigated by Sheiko et al. [104, 105] and Coen et al. [106]. Bar et al. [107] have prepared dendrimer-modified silicon oxide surfaces and used them as a platform for the deposition of gold and silver colloid monolayers. The thermodynamics and kinetics of adsorption of redox-active dendrimers, containing ferrocenyl moieties on the periphery, have been studied on a Pt electrode surface [108]. Adsorption isotherm depended on the applied potential. At the potential where the ferrocenyl sites are in the reduced form, the adsorption thermodynamics were characterized by the Langmuir adsorption isotherm. When the ferrocenyl sites are oxidized, the electrodeposition of a multilayer of the dendrimer took place. Focally substituted organothiol dendrons were used to construct self-assembled adlayers on a gold surface [109]. As the number of hyperbranches in the dendron increases, the dendron adlayers become more permeable, indicating a tradeoff between size and the packing efficiency. This research suggests the formation of homogeneous but permeable dendron adlayers on the gold surface. Díaz et al. [110] have reported the interfacial reaction of the terpyridyl-pendant dendrimers with Fe^{2+} and Co^{2+} on highly oriented pyrolytic graphite surfaces. The films form highly ordered, two-dimensional hexagonal arrays, which appear to be composed of one-dimensional polymeric strands. The dimensions obtained are consistent with the size of the dendrimer. The ordering in the dendrimer film is dependent on the dendrimer generation. The films are electrochemically active. Sabapathy and Crooks [111] have prepared a hydroxyl-terminated monolayer from fourth generation PAMAM dendrimer and reacted it with heptanoyl chloride to yield ester-coupled bilayers. The interfacial reactivity was discussed in relation to the monolayer structure and the intrinsic properties of the particular coupling reaction studied. The lateral organization of alkyl-substituted polyphenylene dendrimers on the basal plane of graphite has been investigated by Loi et al. [112]. The dendrimers consist of a core of twisted, interlocked benzene rings and an external shell of dodecyl chains. While three kinds of dendrimers show a tetrahedral or a disk-like shape in solution, the dendrimers on graphite spontaneously form a stable, almost pinhole-free monolayer. Complex two-dimensional arrangements and supramolecular ordering were observed in the monolayers prepared by spin-coating. One prominent structure is regions of parallel rows of 6 nm spacing. In addition, pairs of dendrimers formed two-dimensional crystals on graphite. The crystal structure depends sensitively on the structure of the dendrimer, on the solvent, and on the concentration. The interfacial behavior of third and fourth generations of hyperbranched polyesters with hydroxyl-terminal groups was studied by Sidorenko et al. [113]. The molecular adsorption on a bare silicon surface was described in terms of the Langmuir isotherm. A higher adsorption amount was found for a lower generation. The shape of a third generation dendrimer within an adsorbed layer evolved from a pancake within a thickness less than 1 nm for very low surface coverage to densely packed, worm-like bilayer structure with a thickness of about 3 nm for the highest surface coverage. The fourth generation molecules hold a stable close-to-spherical shape with a diameter of 2.5 nm throughout the entire range of surface coverage. The intermolecular flexibility or constrained mobility of dendrimers was considered to be responsible for different surface behavior.

Recently, the morphology of aggregates of dendrimers on the solid substrate was investigated. Sato et al. [114] have reported that dendrimers aggregate in a form of nanometer-sized round dots over an area measured in centimeters on rapid evaporation of a solvent from a thin cast film of an electrolyte solution of poly(amido amine) dendrimers on mica. Chemically specific adsorption, electrostatic interactions, phase transitions, and dewetting instabilities were shown not to be responsible for the dot formation. Changes in temperature and humidity have only little effect. There is a threshold evaporation rate for the formation of dots. Once formed, the dot size and spacing are independent of the evaporation rate. The self-assembly of monodendrons with peripherally attached alkyl substituents has been studied by scanning tunneling microscopy (STM) [115]. The disk-like assembly, a characteristic structure of low-generation dendrimers, was directly observed. The subunits of disk structure can be well resolved as well as the ordered alkyl parts. Xiao et al. [116] have reported organosilane thin films derived on mica surfaces from $SiCl_3$-terminated carbosilane dendrons by means of spin-coating. The morphology of the films was highly dependent upon the generation of the dendrons and the film thickness—mesoscopic ring, disk, or hole structures were observed. These structures were composed of nanoparticles with sizes corresponding to one dendron molecule or the cluster of a few laterally bound molecules. At submonolayer coverage, the molecules tended to flatten and spread out on mica surfaces. The mechanisms for the formation of the observed film morphology were discussed, based on the structure and properties of the dendrons and the effect of the evaporation process.

4.3. Self-Assembled Monolayers

The organized self-assembled monolayers (SAM) of dendrimers were prepared by using a template SAM on substrate. Amine-terminated PAMAM dendrimers were covalent-linked with organized, surface-confined, self-assembled monolayers of mercaptoundecanoic acid [117]. Yoon et al. [118] have also prepared same dendrimer monolayer on acid SAM on gold and then functionalized the dendritic surface amine groups with biotin analogues or desthiobiotin amidocaproate. For testing the association/dissociation reaction cycles at the affinity surface, avidine adlayer was formed onto the biotin analogue-functionalized surface and displaced with free biotin. With

the optimized affinity-surface construction steps and reaction conditions, continuous association/dissociation reaction cycles were achieved, resulting in a repeatedly regenerable affinity-sensing surface. Ionized, carboxylate-terminated polyphenylene dendrimer molecules were adsorbed on a carboxylic acid group-terminated, self-assembled monolayer on a gold substrate through the linkage with Cu^{2+} ions [119]. The strong interaction between dendrimer and Cu^{2+} ions, the latter of which is preadsorbed on the COOH SAM, led to a compression or deformation of the SAM and resulted in a decreased height of the dendrimer ions. Fail et al. [120] have immobilized amine-terminated PAMAM dendrimers onto anhydride-functionalized pulsed plasma polymer surfaces via amide linkage formation. The PAMAM dendrimer layers were useful for a variety of surface-related phenomena of fluorination, adhesion, and gas barrier enhancement.

Nagaoka and Imae [121] have reported adsorption structure of amine-terminated PAMAM dendrimer onto 3-mercaptopropionic acid (MPA) SAM on Au island film. The carboxylic acid species of SAM diminished, as the adsorption of PAMAM dendrimer from an aqueous solution proceeded. This indicates that the protonated, amine terminal groups of the dendrimer bind electrostatically to carboxylate groups of SAM. The flattened molecular structure or the imperfect covering of the adsorbed dendrimers was assumed. The dome-shaped, "spread out" configuration of PAMAM dendrimers on substrate has been visually observed by Li et al. [122].

Adsorption kinetics of fourth generation amine-terminated PAMAM and PPI dendrimers from aqueous solutions has been investigated on MPA SAM on Au film [123]. The adsorption kinetics at high dendrimer concentrations obeyed two-step adsorption process [124] but not Langmuir adsorption isotherm. Then, monolayer and additional adsorptions of dendrimers must occur on MPA SAM. There is a difference on the adsorption structure between two dendrimers, as seen in Figure 7. PAMAM dendrimer adsorbs with "the hemi-micellar structure," as illustrated in Figure 7(a), because amine and amido groups of PAMAM dendrimer interact electrostatically and through hydrogen bonding with carboxylate of MPA SAM. The adsorption

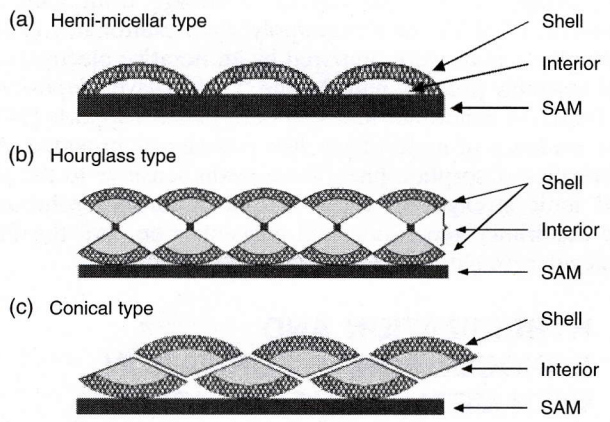

Figure 7. Adsorption models of PAMAM and PPI dendrimers on MPA SAM. Reprinted with permission from [123], H. Nagaoka and T. Imae, *Int. J. Nonlinear Sci. Numer. Simu.* 3, 233 (2002). © 2002, Freund Publishing House Ltd.

structure of PPI dendrimer is "the hour glass type" or "the conical type" (see Fig. 7(b) and (c)), since there is no hydrogen-bonding interaction between dendrimer interior and MPA SAM.

In the case of PAMAM dendrimers, surface-functionalized with ruthenium (II), the adsorption thermodynamics of this redox-active metallodendrimers onto Pt electrodes was well characterized by the Langmuir adsorption isotherm [125]. The adsorption kinetics was found to be activation-controlled with the rate-constant decreasing with decreasing dendrimer generation. The rate of adsorption of positively charged poly(propylene imine) dendrimers on glass, an oppositely charged surface, has been studied as a function of generation and charge [126, 127]. The adsorption kinetics was mostly diffusion/convection-controlled with a linear dependence on the bulk concentration. At high bulk concentration, there is a drop in concentration dependence, and this crossover concentration shifts to higher concentrations with decreasing pH. Bahman et al. [128] have studied *in-situ* adsorption of PAMAM dendrimers from dilute solutions onto cleaned gold. In ethanol, the equilibrium surface coverage corresponds to almost monolayer and increases slightly with generation. The adsorption is likely driven by the weak favorable interaction between the primary amine end groups on PAMAM dendrimer and gold. In aqueous media, under the conditions where the PAMAM amine end groups tend to protonate and bear positive charge, the equilibrium surface coverage grows exponentially with generation, indicating the multilayer formation. The formation of multilayers can be explained by a favorable electrostatic image-charge interaction between the positively charged dendrimers and the gold substrate. At the seventh generation, there was a manifestation of "dense-shell" packing, which lowers the effective charge on the higher generation dendrimers.

Stable ultra-thin self-assembled films were prepared by dendron thiol. Zhang and his collaborators [129, 130] have synthesized polyether dendron with a thiol group at the focal point and used it for the preparation of self-assembled monolayers on metal surface. The dendron SAM covered the gold surface homogeneously and consisted of the ordered stripes by the packing of two flat-cone shaped dendrons. The patterned stripes can be improved by thermal annealing. From the studies of the kinetic process of dendron thiol self-assembling on gold, it was shown that the dendron thiol assembling proceeds with different adsorption rates depending on the assembly time [130]. They have also fabricated ultra-thin organic films via dendritic growth on modified gold, silicon, and quartz substrates [131].

4.4. Composite Films

Investigation was extended to the preparation of composite self-assembled monolayers including dendrimer primarily by Crooks et al. [132–136]. PAMAM dendrimers were surface-immobilized in thiol, self-assembled monolayers by means of two different methods [132], which are the preparation of chemically sensitive dendrimer surfaces as a vapor-phase dosing probe. Zhao et al. [133] have embedded surface-confined dendrimers within self-assembled monolayers of alkane thiol. These films act as ion gates of molecular dimension. The two-dimensional

phase behavior of mixed monolayers composed of amine-terminated PAMAM dendrimers and n-alkylthiols has been studied by Lackowski et al. [134]. Mixed monolayers were prepared by sequential immersion of Au substrates in ethanolic solutions of dendrimers and then n-alkylthiols. Time-dependent morphological changes were observed in the mixed monolayers. Dendrimer monolayers immersed in a hexane solution of n-alkylthiols did not phase-separate to an appreciable extent. Moreover, thiol-terminated dendrimers did not phase-separate either, when exposed to ethanolic n-alkylthiol solutions. It was suggested that one of the driving forces for the phase segregation in the mixed monolayers is the difference in adsorption energies of the amine and thiol groups against the Au substrate. Tokuhisa et al. [135] have reported that exposure of high-generation dendrimer monolayers to ethanoic solutions of hexadecanethiol results in a dramatic compression of the dendrimers and causes them to reorient on the surface from an oblate to prolate configuration without desorb. It was shown that the primary driving force for the structural change is the solvation of the dendrimers. Oh et al. [136] have recently described a strategy for constructing a dendrimer-based electrochemical current rectifier permitting current flow in only one direction. The dendrimer-based rectifying layer was prepared by direct adsorption of ferrocene-functionalized poly(propylene imine) dendrimers onto Au surfaces, followed by adsorption of n-hexadecanethiol. The surface coverage of ferrocenyl dendrimers in the two-component monolayers is estimated to be about 50% of maximum coverage. It was revealed that the ferrocenyl dendrimer/n-alkanethiol-modified electrodes exhibit excellent barrier properties, which prevent direct oxidation/reduction of the solution-phase redox molecules. Electrochemical current rectification occurred via mediated electron transfer across the surface-confined ferrocenyl dendrimers. Friggeri et al. [137] have investigated the insertion process of individual, dendrimer sulfide molecules into self-assembled monolayers of 11-mercapto-1-undecanol. The immersion of thiol self-assembled monolayers in a dendrimer solution of increasing concentrations at longer immersion times leads an increase in the dendrimer number inserted into the thiol layer. A mechanism consists of rapid dissociation of surface thiols and follows slow dendrimer adsorption. The rate-determining step of the process is the insertion of the individual dendrimer molecules. On the dissociation step, first-order kinetics was found for the fraction of covered substrate versus time of exposure to solvent.

Layer-by-layer composite films were also prepared. Electrostatic layer-by-layer composite deposition films were fabricated by mutual self-assembly of dendritic macromolecules of two adjacent generations [138]. The formation of layer-by-layer composite films on cationic SAM has carried out by the stepwise adsorption of two PAMAM dendrimers among amine-, carboxylate-, and hydroxyl-terminated species, and is compared with the competitive adsorption of the same paired dendrimers in aqueous solutions [139]. There was apparent conformational change of hydroxyl-terminated dendrimers in the first layer by the accumulated adsorption of amine- or carboxyl-terminated dendrimers, as seen in Figure 8. Normal layer-by-layer accumulation was formed in other combinations of two dendrimers in three species.

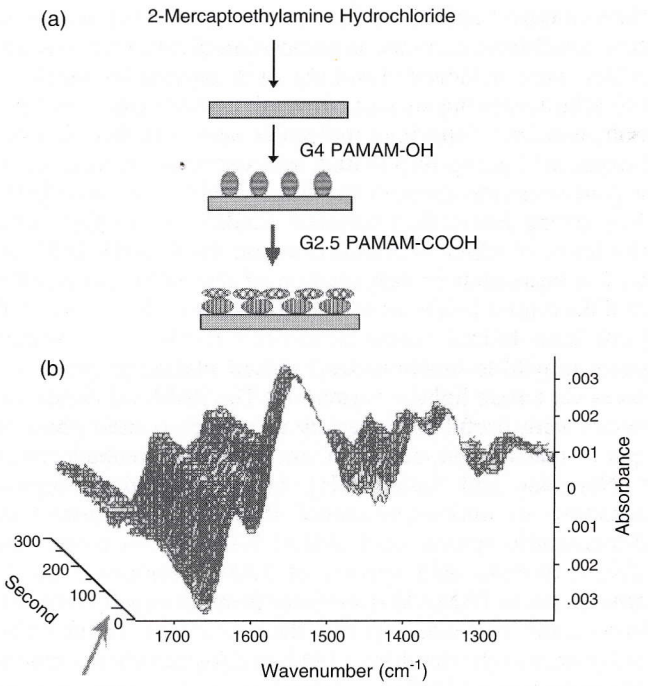

Figure 8. Stepwise adsorption of carboxylate and hydroxyl-terminated dendrimers on 2-mercaptoethylamine hydrochloride SAM. After the adsorption equilibrium of 4th generation hydroxyl-terminated PAMAM dendrimer was attained, the desorption of adlayer in water was equilibrated. The adlayer after the desorption equilibrium was used for the adsorption of 2.5th generation carboxyl-terminated PAMAM dendrimer. (a) Scheme of the stepwise adsorption; (b) the *in-situ* observation of adsorption of 2.5th generation carboxyl terminated PAMAM dendrimer on the adlayer of 4th generation hydroxyl-terminated PAMAM dendrimer. The absorption bands of amide II and OH bending vibrations on attenuated total reflection surface-enhanced infrared absorption spectroscopy decreased in intensity, after the adsorption of carboxylate terminated dendrimer started.

Wang et al. [140] have constructed a photosensitive, layer-by-layered, self-assembled, ultra-thin film based on polyanionic PAMAM dendrimer (with carboxylate terminals) and polycationic nitrocontaining diazoresin via sequential deposition and subsequent UV irradiation, which causes the linkage between the layers to change from ionic to covalent. PAMAM dendrimer/poly(styrenesulfonate) (PSS) multiplayer films were prepared by an iterative electrostatic self-assembly process, namely, the layer-by-layer deposition of PAMAM dendrimer and PSS onto planar supports [141]. The evidence of multi-player film growth was provided. An adsorption-desorption phenomenon was sensitive to the pH and ionic strength of the PSS and dendrimer solutions, the dendrimer generation and concentration, and the PSS molecular weight and concentration.

5. HYBRIDIZATION AND NANOCOMPOSITE FORMATION WITH METAL NANOPARTICLES

Clusters of metals and semiconductors are focused due to their unique mechanical, electronic, optical, magnetic, and chemical properties. Metal nanoparticles are also investigated because of their novel optical, electrical, catalytic, and

other properties. Homogeneous, self-assembled monolayers or thin films of alkanethiol, N-hexadecylethylenediamine [142], polymer [143, 144], polymerized methyl methacrylate [145], hydrophobically modified dendrimers [146–150] have been used as stabilizers in the synthesis of stable hydrophobic nanoparticles. On the other hand, the synthesis of water-soluble hydrophilic particles is recently required in relation to the environmental pollution. Then, water-soluble dendrimers were focused as valuable materials for the protection of clusters and nanoparticles.

Zhao et al. [151] and Balogh and Tomalia [152] have introduced a template-synthesis strategy for preparing copper nanoclusters within dendrimer nanoreactors. Transition metal ions are condensed into the interior of a fourth generation PAMAM dendrimer and chemically reduced to zerovalent copper. Nanocomposite clusters prepared ranged in size from 4 to 64 atoms [151]. The surface properties of the host dendrimers seem to determine the solubility of the metal domains [152].

Esumi et al. [153] have prepared gold colloids by the reduction of metal salt by means of ultraviolet irradiation in the presence of zero to fifth generation PAMAM dendrimers with amine terminals. The average particle sizes decreased by increasing the concentration of dendrimers, and gold colloids with a diameter less than 1 nm were obtained in the presence of third to fifth generation dendrimers above the molar ratio of amine group of dendrimer: $HAuCl_4 = 4 : 1$. Sugar-persubstituted PAMAM dendrimers (sugar balls) were also used for the spontaneous formation of gold nanoparticles [154]. Au^{3+} ions were reduced by the hydroxyl groups of the sugar balls, resulting in the formation of very stable gold nanoparticles. Garcia et al. [155] have stated that large dendrimers encapsulate the colloids and lower-generation dendrimers give rise to larger colloids. Fourth-generation PAMAM dendrimers having terminals functionalized with thiol groups have been synthesized by Chechik and Crooks [156]. While these thiolated dendrimers formed stable monolayers on planar Au substrates, the reduction of $HAuCl_4$ in the presence of thiol-modified dendrimers resulted in the formation of water-soluble, dendrimer-stabilized nanoparticles with 1.5–2.1 nm in diameter. Stable nanoparticles were obtained at Au/dendrimer ratios as large as 120:1.

Esumi et al. [157] have compared the role of generations (third to fifth generation) and terminal groups (amine and carboxyl) of PAMAM dendrimers for preparing nanoparticles of gold, platinum, and silver. Whereas the size of gold and silver nanoparticles decreased with increasing the concentration and the generation of dendrimers, the size of platinum nanoparticles was insensitive against the concentration as well as the generation. Stable nanoparticles were obtained above unity of the ratio of surface group of dendrimer/metal salt for gold and silver nanoparticles and above 40 for platinum nanoparticles. It was suggested that the metal nanoparticles adsorb on the exteriors of the dendrimers.

Manna et al. [158] have synthesized silver and gold nanospherical particles stabilized by a fourth-generation, amine-terminated PAMAM dendrimer by the reduction of $AgNO_3$ and $NaAuCl_4$. The particle size could be controlled by the metal ion-to-dendrimer mixing ratio. Silver nanoparticles are always larger than gold nanoparticles, when they are synthesized by the same condition. A short-ranged hexagonal arrangement of particles was observed in a monolayer onto a carbon-coated copper transmission electron microscopic grid. Then, the terminal amine groups of the dendrimers take part in the stabilization of the nanoparticles, and the dendrimers protecting nanoparticles behave as a spacer packed between the ordered arrangements of the nanoparticles.

PAMAM denderimers with amine terminals possess both internal and external functional groups providing reaction sites for metal ions. Then, it is very important in the application that nanoparticles are either formed in the interior of dendrimers or at the external surface of dendrimers. The previous reports indicated that the hybrid structures of dendrimer-metal nanoparticles depend on the generation, concentration, and terminal group of dendrimers, the type of metals, and the ratio of dendrimers and metals. Gröhn et al. [149, 159, 160] have clarified the influence of reaction conditions and dendrimer generation on the resulting nanostructures of dendrimer-metal hybrid colloids. Second to fourth generation PAMAM dendrimers behave like colloid stabilizers; that is, several dendrimers surround the surface of the metal particle, as shown in Figure 9. On the other hand, sixth to tenth dendrimers act as effective nanotemplates. Then, metal particles are completely formed inside individual dendrimers. Gröhn et al. [160] have prepared hydrophilic polymer networks containing higher generation PAMAM dendrimers, where nanoparticles are located inside. Crooks et al. [161] have used hydroxyl-terminated PAMAM dendrimers for the preparation of metal nanoparticles in the interior of dendrimers, because the dendrimers do not have functional terminal groups as reaction sites for metal ions. They reviewed synthesis and characterization of dendrimer-encapsulated metal nanoparticles and their applications to catalysis. Recently, Ottaviani et al. [162] have achieved the transformation of silver from Ag^+ to Ag^0 in the interior of dendrimer by irradiating the solution of Ag^+-dendrimer complex by means of an excessive dose of X-rays to avoid alternation of the

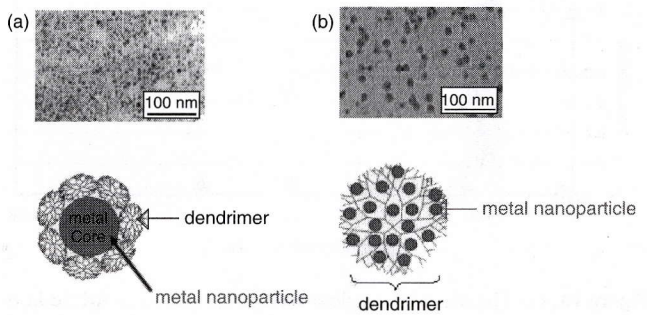

Figure 9. Transmission electron microscopic (TEM) photographs and models of dendrimer-passivated and dendrimer-encapsulated nanoparticles. TEM: (a) deposition on a carbon-coated cupper grid of 4th generation amine-terminated PAMAM dendrimer-passivated gold nanoparticles prepared at the 1:10 ratio for the Au atom:terminal amine group of dendrimer; (b) dendrimer-encapsulated nanoparticles. Reprinted with permission from [159], F. Gröhn et al., *Macromolecules* 33, 6042 (2000). © 2000, American Chemical Society.

structure of the complexes during transformation into nanocomposites.

High stability of dendrimers surrounding the surface of the metal particles is indispensable not only in the protection of particles but also in the utilization of particles. We have investigated the exchange of dendrimers on gold nanoparticles by dodecanethiols at various mixing ratios of nanoparticle and dodecanethiol. The wine-red aqueous solution of dendrimer-passivated gold nanoparticles was vigorously shaken with an n-heptane or diethyl ether solution of dodecanethiols, until the exchange equilibrium was reached. When two phases were separated into the upper organic and lower aqueous phases, wine-red color shifted into organic phase. Figure 10(a) shows the absorption spectra of the water and n-heptane phases after the exchange reaction. The plasmon band (around 510 nm) intensity of nanoparticles in the aqueous phase decreased with the exchange and, at the same time, the band intensity in n-haptane phase increased. The intensity variation of the plasmon band as a function of the mixing ratio of dodecanethiol to gold ions is plotted in Figure 10(b). Although the average particle sizes are maintained even after the exchange reaction, the infrared absorption spectroscopic vibration bands of dendrimers exchanged by absorption bands of dodecanethiol.

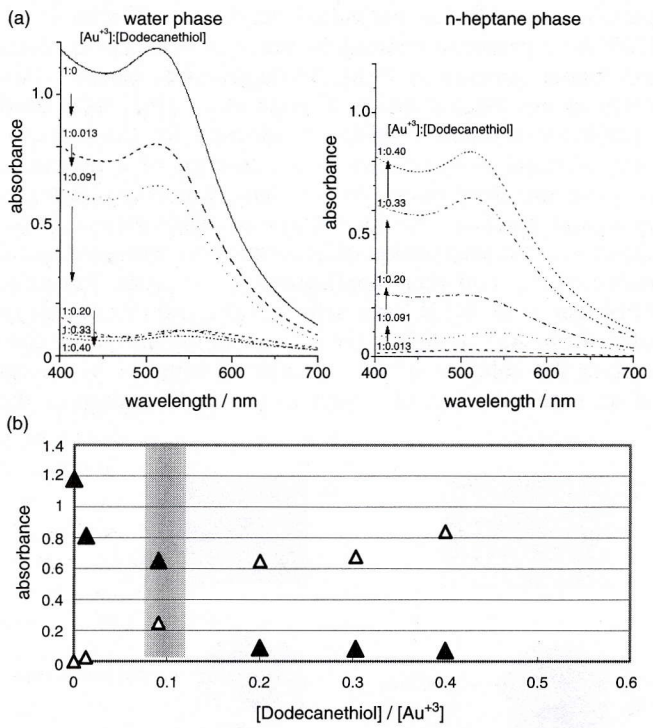

Figure 10. (a) The ultraviolet-visible absorption spectra of hybrid-layer-passivated nanoparticles in water and in n-hexane phases after the ligand replacement reaction at the different ratios of dodecanethiol against Au atom, [dodecanthiol]/[Au^{3+}]. Dendrimer-passivated gold nanoparticles in water and dodecanethiol in n-heptane were shaken until the equilibrium was reached, and the water phase was separated from the n-heptane phase. (b) Plasmon band intensity, as a function of [dodecanthiol]/[Au^{3+}] in water phase (▲) and in n-heptane phase (△) after the ligand replacement reaction. In the shadowed region, solutions of both phases colored.

Although the exchange of dendrimer by dodecanethiol in diethyl ether solution proceeded as well as in n-heptane solution, dendrimer on nanoparticles did not exchange with N-hexadecylethylenediamine in n-heptane solution. On the other hand, N-hexadecylethylenediamine, which was passivated on gold nanoparticles in n-heptane solution, also did not exchange with free dendrimer in water. (N-hexadecylethylenediamine-passivated gold nanoparticles were prepared according to the procedure previously reported for the preparation of silver nanoparticles [142].) The ligand replacement reaction is schematically illustrated in Figure 11. The replacement by the addition of a small amount of dodecanethiol indicates that the interaction of a gold particle surface with amine terminal groups of the dendrimer is weaker than that with thiol. However, the interaction of dendrimer and N-hexadecylethylenediamine on gold nanoparticle surface cannot be discriminated.

In the process of the replacement of dendrimer-passivated nanoparticles by dodecanethiols, gold nanoparticles, surface-confirmed by hybrid self-assembled monolayers, was synthesized in the mixing ratio shadowed in Figure 10(b), where both solutions of water and organic solvent were colored. The formation of the hybrid monolayer is very feasible by the partial replacement of surface-confined dendrimer onto the gold particle surface. The hybrid-layer-passivated nanoparticles separated into domains of small and large spheres [163]. That is, the change of the hydrophilic particle surface to the amphiphilic one induces the segregation into the close-packed monodispersed phases. This indicates that the replacement may be dependent on the particle size. The potentialities of nanoparticles stabilized by hybrid monolayers of fascinating molecules, such as dendritic polymers and surfactants, may be high as well as those of the homogeneous ones. Thus, the hydrophilic/hydrophobic hybrid-layer-protected nanoparticles may stimulate the new development of fundamental surface sciences and new applications of such nanoparticles on chemical sensing, catalysis,

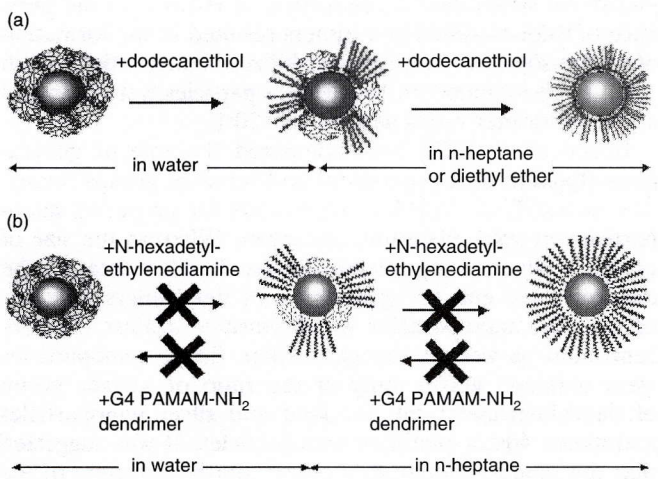

Figure 11. The schematic presentation of ligand replacement reaction. (a) Dendrimer-passivated gold nanoparticles in water + dodecanethiol in n-heptane or diethyl ether. (b) Dendrimer-passivated gold nanoparticles in water + N-hexadecylethylenediamine in n-heptane and N-hexadecylethylenediamine-passivated gold nanoparticles in n-heptane + dendrimer in water.

coating, etc., different from homogeneous hydrophobic or hydrophilic nanoparticles.

Esumi and Goino [164] have reported the adsorption of PAMAM dendrimer on alumina and silica particles at pH 5. The adsorption of dendrimers with surface ionic groups on oppositely charged particles increased with increasing dendrimer generation. While the earlier generation dendrimers behave as ordinary electrolytes, the later generation dendrimers behave as ionic surfactant or polyelectrolyte for the inorganic particle dispersion. The adsorption amounts of dendrimers with carboxylate terminals were greater than those with amine terminals. Esumi et al. [165, 166] have investigated the simultaneous adsorption of PAMAM dendrimers and anionic surfactants on positively charged alumina particles. There was competitive adsorption between the dendrimers with carboxylate terminal groups and sodium dodecyl sulfate at pH 5 [165]. A preferential adsorption of 5.5th generation over 1.5th generation was also observed in the competitive adsorption with anionic surfactant. The adsorption amount of sugar-persubstituted poly(amido amine) dendrimers, sugar balls, at pH 3.5 changes through a maximum, while the adsorption of anionic surfactant increases with increasing it [166]. The enhancement in the simultaneous adsorption is due to the adsorption of complexes consisting of sugar ball and anionic surfactant. In addition, the dispersion stability of alumina suspensions, which was caused by the adsorption of the sugar ball and anionic surfactant, depends on the zeta potential of alumina. The generation of sugar ball and the kind of anionic surfactant did not significantly influence the adsorption characteristics.

There are very few reports of nanocomposites of dendrimers with nanoparticles except metal nanoparticles. Naka et al. [167] have carried out the crystallization of $CaCO_3$ in the presence of PAMAM dendrimer containing carboxylate groups at the external surface. Spherical vaterite crystals were formed, different from the formation of rhombohedral calcite crystals in the absence of additives. CdS in PAMAM dendrimer solutions precipitated as aggregates composed of dendrimer-stabilized nanoclusters with long-term optical stability [168]. Kinetics for the growth of aggregates was discussed—temperature and reactant concentration are dominant variables controlling the aggregation kinetics.

6. CONCLUSIONS

Applications of dendrimers, in connection with the novel characters of dendrimers, are considered in the field of not only industry but also life science. Concerning the doping ability, one of the potentials for the use of PAMAM dendrimers, which are adaptable to native bodies, is biomedical application as magnetic resonance imaging (MRI) contrast agents and drug delivery for diagnoses [5, 7]. Recently, the potentials of water-soluble dendritic unimolecular micelles as drug delivery agents were explored using a model drug—indomethacin [169]. Entrapment of indomethacin in the dendritic micelles was achieved at 11 wt % loading content, and preliminary *in-vitro* release tests showed that sustained release characteristics were achieved. This study supports the possible application of dendritic unimolecular micelles with a hydrophobic core and a hydrophilic shell in drug delivery and suggests the necessary construction of dendrimers with possible structures to optimize chemical, physical, and pharmacological properties.

For the complexiation of PAMAM dendrimers with DNA, which is a mimicry of nucleohistone, the utilization as gene deliverer or vector is examined. Moreover, the complexiation ability of ionic dendrimers with polyelectrolytes may be relevant for applications in polymer separation and viscosity control. The extension of complexiation investigation of dendrimers with linear polyelectrolytes is the formation of gels and networks using dendrimers as building blocks. Amphiphilic hydrogels with highly shaped persistent cross-link junctions were synthesized using linear blocks and perfectly branched (dendritic) macromolecules [170]. The swelling of the gels formed is affected by the relative content of linear polymer, the polarity of the medium, and the temperature. In the preparation of the hydrogels, the influence of various factors on the degree of crystallinity and phase segregation must be considered. Covalently cross-linked, three-dimensional nano-domained networks were prepared from radially layered poly(amido amine-organosilicon) copolymers containing hydrophilic PAMAM dendrimer interiors and reactive organosilicon exteriors [171]. Sizes and shapes of the nanoscopic domains can be controlled by the selection of dendrimer network precursors and by conditions applied to the network conformation.

Architectures of dendrimers designed at the molecular level on interfaces are developed for the purpose of manifold applications such as molecular, chemical, biomimetic, electronic, photochromic, and pH-sensitive sensors or devices. Then, the dendrimer molecules that produce stable, functional, and select interfacial architectures as nanoreactors and nanoreservoirs are exploited as many nanoscopic smart materials or their building blocks, including molecular deliveries, segregations, reaction catalysts, transport agents, and molecular recognitions. The sensitive and selective sensor layers were prepared from polyphenylene dendrimers and used to monitor the concentration of various organic compounds in different environments [172]. The homogeneous, rigid layers of polyphenylene dendrimers allowed the selective detection with high sensitivity and accuracy of polar aromatic target molecules. This is comparable to the benzamido-terminated PAMAM dendrimer-type gas sensor [132]. This sensor probed volatile, organic molecules of heptane, carbon tetrachloride, trichloroethylene, benzene, and 1-buthanol. These types of sensors should be of increasing significance in environmental science. The difference of microcavities between two dendrimers was elucidated using solvatochromic probe, phenol blue [173]. Fluorescence sensing a 2.5th generation PAMAM dendrimer with a naphthalene core unit was prepared, and its potential use as a pH sensor material was examined [174]. It displayed sensitive fluorescence signal amplification towards tetrafluoroacetic acid in comparison to acetic acid. It is then demonstrated that the effects of chemical structural differences of dendrimers are essential as selective sensing probe for different target molecules, and the design and synthesis of more elaborate dendrimers are a fascinating challenge for fabricating the best sensors.

Recently, the preparation of patterned thin films including dendrimers was reported [175–178]. The soft lithographic technique, microcontact-printing method, was used to transfer patterned thin films to surfaces with submicrometer resolution [175]. The fourth-generation amine-terminated PAMAM dendrimers were used as the "ink" molecules. Stable multilayer structures up to roughly 60 nm in height were prepared from dendrimer solutions of high concentrations. The deposition of gold-containing dendrimers on stripe-patterned self-assembled monolayer substrates was studied using the microcontact printing method [176]. The atomic force microscopic (AFM) image showed that the PAMAM dendrimers are selectively deposited on hydrophilic –COOH stripes of the patterned substrates but not on the hydrophobic $-CH_3$ stripes. Arbitrary submicrometer patterns of cobalt were fabricated on a nonconducting surface with wet chemical and microcontact printing methods [177]. A hydroxyl-terminated dendrimer was transferred from a stamp to the surface. The guests, palladium ions, adsorbed into the dendrimer layer as host and acted as nucleation centers for electroless cobalt plating. Patterned dendrimer/gold nanoparticles, immobilized on polymeric substrates, were prepared by masking a patterning method [178]. Polymer substrate, such as poly(dimethylsiloxane) or poly(ethyleneterephthalate) film, was plasma-treated with maleic anhydride. The resulting succinic anhydride groups on the surface were reacted with amine groups of PAMAM dendrimers containing gold salts. The film was irradiated with ultraviolet light through a photomask. The gold particles were well patterned on the surface of the polymer film.

New families of nanocomposite clusters and particles were synthesized. Nanoscale super clusters, assembled around a dendritic core, were synthesized and characterized as quantum dots [179]. Compounds were prepared by binding cluster units $[Ru_5C(CO)_{12}]$ or $[Au_2Ru_6C(CO)_{16}]$ to third-generation dendrimers. Those show a molecular multi-layer structure, which is viewed as a sphere consisting of a nonconducting dendritic core with a sheath of conducting metal clusters over the surface and, in turn, being covered by an additional outer layer of insulating carboxyl ligands. Their properties suggest that they may be of use in a gas delivery/storage system switched thermally or electrochemically, delivering metal particles of precise nuclearity for nanoelctronics and catalysis. Polymerization of styrene in aqueous dispersions of sodium dodecyl sulfate and PPI dendrimer with initiation by potassium persulfide at 80 °C produced latexes [180]. Microscopic observation showed independent particles with diameters of 26–64 nm and small clusters.

GLOSSARY

Dendrimer Spherical polymer prepared by covalent-bonding from a functional core through the successive repeating synthesis of a spacer and a branching part.

Deoxyribonucleic acid (DNA) A biopolymer consisting of two polynucleotide chains with the sugar-phosphate backbones. Two chains forming right-handed helices run in opposite direction.

Lamellar layer One type of lyotropic liquid crystals constructed by surfactant molecules. Molecules are associated into accumulates of bilayers with hydrophobic and hydrophilic spaces.

Linear polymer Molecule with high-molecular-weight which was prepared by the polymerization of bifunctional monomers.

Self-assembled monolayer Monolayer formed by the interaction (covalent bond) of adsorbed molecules with the substrate.

Sodium hyarulonate Native polysaccharide of the glucosamminoglycan family, which is composed of alternating units of D-glucuronic acid and N-acetyl-D-glucosamine.

Sodium poly-L-glutamate Polypeptide composed of L-glutamic acid which is one of components of protein. It takes structures of α-helix, β-form and random coil, depending on the condition.

REFERENCES

1. D. A. Tomalia, A. M. Naylor, and W. A. Goddard, III, *Angew. Chem. Int. Ed.* 29, 138 (1990); *Angew. Chem.* 102, 119 (1990).
2. J. M. J. Fréchet and C. J. Hawker, in "Comprehensive Polymer Science," 2nd suppl. (G. Allen, Ed.). Elsevier Science, Pergamon, Oxford, 1996.
3. G. R. Newkome, C. N. Moorefield, and F. Vögtle, "Dendritic Molecules: Concepts, Synthesis, Perspectives." VCH, Weinheim, 1996.
4. F. Zeng and S. C. Zimmerman, *Chem. Rev.* 97, 1681 (1997).
5. M. Fischer and F. Vögtle, *Angew. Chem. Int. Ed.* 38, 884 (1999).
6. V. Percec and M. N. Holerca, *Biomacromolecules* 1, 6 (2000).
7. R. Esfand and D. A. Tomalia, *DDT* 6, 427 (2001).
8. F. Vögtle, "Dendrimers III Design, Dimension, Function, 212 Topics in Current Chemistry." Springer, Berlin, 2001.
9. G. Caminanti, N. J. Turro, and D. A. Tomalia, *J. Am. Chem. Soc.* 112, 8515 (1990).
10. C. Honda, M. Itagaki, R. Takeda, and K. Endo, *Langmuir* 18, 1999 (2002).
11. J.-H. Kim, M. M. Domach, and R. D. Tilton, *Langmuir* 16, 10037 (2000).
12. G. Pistolis, A. Milliartis, C. M. Paleos, and D. Tsiourvas, *Langmuir* 13, 5870 (1997).
13. G. Pistolis and A. Milliartis, *Langmuir* 18, 246 (2002).
14. A. Schmitzer, E. Perez, I. Rico-Lattes, A. Lattes, and S. Rosca, *Langmuir* 15, 4397 (1999).
15. Y. Pan and W. T. Ford, *Macromolecules* 33, 3731 (2000).
16. D. Leisner and T. Imae, *J. Phys. Chem. B* 197, 8098 (2003).
17. W. Chen, D. A. Tomalia, and J. L. Thomas, *Macromolecules* 33, 9169 (2000).
18. S. Jockusch, J. Ramirez, K. Sanghvi, R. Nociti, N. J. Turro, and D. A. Tomalia, *Macromolecules* 32, 4419 (1999).
19. I. B. Bietveld, W. G. Bouwman, M. W. P. L. Baars, and R. K. Heenan, *Macromolecules* 34, 8380 (2001).
20. K. Funayama, T. Imae, K. Aoi, K. Tsutsumiuchi, M. Okada, M. Furusaka, and M. Nagao, *J. Phys. Chem. B* 107, 1532 (2003).
21. Y. Chang, Y. C. Kwon, S. C. Lee, and C. Kim, *Macromolecules* 33, 4496 (2000).
22. L. A. Baker and R. M. Crooks, *Macromolecules* 33, 9034 (2000).
23. U. Oertel, D. Appelhans, P. Friedel, D. Jehnichen, H. Komber, B. Pilch, B. Hänel, and B. Voit, *Langmuir* 18, 105 (2002).
24. C. J. Hawker and J. M. J. Fréchet, *J. Am. Chem. Soc.* 112, 7638 (1990).
25. N. C. Greenham, S. C. Moratti, D. D. C. Bradley, R. H. Friend, and A. B. Holmes, *Nature* 365, 628 (1993).

26. C. J. Hawker, K. L. Woley, and J. M. J. Fréchet, *Chem. Soc. Perkin. Trans. Part 1*, 1287 (1993).
27. J. M. J. Fréchet, *Science* 263, 1710 (1994).
28. M. Antonietti and C. Goltner, *Angew. Chem. Int. Ed. Engl.* 36, 910 (1997).
29. M. Zhao, L. Sun, and R. M. Crooks, *J. Am. Chem. Soc.* 120, 4877 (1998).
30. L. Balogh and D. A. Tomalia, *J. Am. Chem. Soc.* 120, 7355 (1998).
31. C. Plank, K. Mechtler, F. C. Szoka, Jr., and E. Wagner, *Human Gene Therapy 7*, 1437 (1996).
32. J. F. Kukowska-Latallo, A. U. Bielinska, J. Johnson, R. Spindler, D. A. Tomalia, and J. R. Baker, Jr., *Proc. Natl. Acad. Sci. USA* 93, 4897 (1996).
33. A. U. Bielinska, J. F. Kukowska-Latallo, J. Johnson, D. A. Tomalia, and J. R. Baker, Jr., *Nucl. Acids Res.* 24, 2176 (1996).
34. M. X. Tang, C. T. Redemann, and F. C. Szoka, Jr., *Bioconjugate Chem.* 7, 703 (1996).
35. C. L. Gebhart and A. V. Kabanov, *J. Control Rel.* 73, 401 (2001).
36. D. Luo, K. Haverstick, N. Belcheva, F. Han, and W. M. Saltzman, *Macromolecules* 35, 3456 (2002).
37. M. F. Ottaviani, B. Sacchi, N. J. Turro, W. Chen, S. Jockusch, and D. A. Tomalia, *Macromolecules* 32, 2275 (1999).
38. M. F. Ottaviani, F. Furini, A. Casini, N. J. Turro, S. Jockusch, D. A. Tomalia, and L. Messori, *Macromolecules* 33, 7842 (2000).
39. W. Chen, N. J. Turro, and D. A. Tomalia, *Langmuir* 16, 15 (2000).
40. V. A. Kabanov, V. G. Sergeyev, O. A. Pyshkina, A. A. Zinchenko, A. B. Zezin, J. G. H. Joosten, J. Brackman, and K. Yoshikawa, *Macromolecules* 33, 9587 (2000).
41. A. U. Bielinska, J. F. Kukowska-Latallo, and J. R. Baker, Jr., *Biochim. Biophys. Acta* 1353, 180 (1997).
42. A. Mitra and T. Imae, *Biomacromolecules*, in press.
43. T. Imae, T. Hirota, K. Funayama, K. Aoi, and M. Okada, *J. Coll. Interf. Sci.* 263, 306 (2003).
44. Y. Li, P. L. Dubin, R. Spindler, and D. A. Tomalia, *Macromolecules* 28, 8426 (1995).
45. H. Zhang, P. L. Dubin, R. Spindler, and D. A. Tomalia, *Ber. Bunsenges. Phys. Chem.* 100, 923 (1996).
46. H. Zhang, P. L. Dubin, J. Ray, G. S. Manning, C. N. Moorefield, and G. R. Newkome, *J. Phys. Chem. B* 103, 2347 (1999).
47. N. Miura, P. L. Dubin, C. N. Moorefield, and G. R. Newkome, *Langmuir* 15, 4245 (1999).
48. V. A. Kabanov, A. B. Zezin, V. B. Rogacheva, Zh. G. Gulyaeva, M. F. Zansochova, J. G. H. Joosten, and J. Brackman, *Macromolecules* 32, 1904 (1999).
49. T. Imae and A. Miura, *J. Phys. Chem. B* 107, 8088 (2003).
50. P. Chodanowski and S. Stoll, *Macromolecules* 34, 2320 (2001).
51. S. Stoll and P. Chodanowski, *Macromolecules* 35, 9556 (2002).
52. J. Xia, H. Zhang, D. R. Rigsbee, P. Dubin, and T. Shaikh, *Macromolecules* 26, 2759 (1993).
53. P. Welch and M. Muthukumar, *Macromolecules* 33, 6159 (2000).
54. S. H. Chen and T. L. Lin, *Methods Exp. Phys.* 23, 489 (1987).
55. T. Imae, K. Funayama, K. Aoi, K. Tsutsumiuchi, M. Okada, and M. Furusaka, *Langmuir* 15, 4076 (1999).
56. K. Funayama and T. Imae, *J. Phys. Chem. Solids* 60, 1355 (1999).
57. K. Funayama, T. Imae, K. Aoi, K. Tsutsumiuchi, M. Okada, H. Seto, and M. Nagao, *J. Phys. Soc. Jpn.* 70, 326 (2001).
58. S. Komura, H. Seto, and T. Takeda, *Progr. Colloid Polym. Sci.* 106, 1 (1997).
59. H. Matsuoka, Y. Yamamoto, M. Nakano, H. Endo, H. Yamaoka, R. Zorn, M. Monkenbusch, D. Richter, H. Seto, Y. Kawabata, and M. Nagao, *Langmuir* 16, 9177 (2000).
60. K. Funayama, T. Imae, H. Seto, K. Aoi, K. Tsutsumiuchi, M. Okada, M. Nagao, and M. Furusaka, *J. Phys. Chem. B* 107, 1353 (2003).
61. D. Leisner and T. Imae, *J. Phys. Chem. B*, in press.
62. V. Percec, C.-H. Ahn, G. Ungar, D. J. P. Yeardley, M. Möller, and S. S. Sheiko, *Nature* 391, 161 (1998).
63. V. Percec and M. Kawasumi, *Macromolecules* 25, 3843 (1992).
64. V. Percec, P. Chu, and M. Kawasumi, *Macromolecules* 27, 4441 (1994).
65. Z. Bao, K. R. Amundson, and A. J. Lovinger, *Macromolecules* 31, 8647 (1998).
66. S. D. Hudson, H.-T. Jung, V. Percec, W.-D. Cho, G. Johansson, G. Ungar, and V. S. K. Balagurusamy, *Science* 278, 449 (1997).
67. H.-T. Jung, S. O. Kim, Y. K. Ko, D. K. Yoon, S. D. Hudson, V. Percec, M. N. Holerca, W.-D. Cho, and P. E. Mosier, *Macromolecules* 35, 3717 (2002).
68. D. Tsiourvas, T. Felekis, Z. Sideratou, and C. M. Paleos, *Macromolecules* 35, 6466 (2002).
69. Z. Liu, L. Zhu, Z. Shen, W. Zhou, S. Z. D. Cheng, V. Percec, and G. Ungar, *Macromolecules* 35, 9426 (2002).
70. X. Li, T. Imae, D. Leisner, and M. A. López-Quintela, *J. Phys. Chem. B* 106, 12170 (2002).
71. N. J. Caminati, N. J. Turro, and D. A. Tomalia, *J. Am. Chem. Soc.* 112, 8515 (1990).
72. D. M. Watkins, Y. Sayed-Sweet, J. W. Klimash, N. J. Turro, and D. A. Tomalia, *Langmuir* 13, 3136 (1997).
73. S. M. Ghoreishi, Y. Li, J. F. Holtzwarth, E. Khoshdel, J. Warr, D. M. Bloor, and E. Why-Jones, *Langmuir* 15, 1938 (1999).
74. M. Miyazaki, K. Torigoe, and K. Esumi, *Langmuir* 16, 1522 (2000).
75. X. Li, X. He, A. C. H. Ng, C. Wu, and D. K. P. Ng, *Macromolecules* 33, 2119 (2000).
76. Y. Li, C. A. McMillan, D. M. Bloor, J. Penfold, J. Warr, J. F. Holzwarth, and E. Wyn-Jones, *Langmuir* 16, 7999 (2001).
77. M. F. Ottaviani, R. Daddi, M. Brustolon, N. J. Turro, and D. A. Tomalia, *Langmuir* 15, 1973 (1980).
78. M. F. Ottaviani, P. Favuzza, B. Sacchi, N. J. Turro, S. Jockusch, and D. A. Tomalia, *Langmuir* 18, 2347 (2002).
79. S. E. Friberg, M. Podzimek, D. A. Tomalia, and D. M. Hedstrand, *Mol. Cryst. Liq. Cryst.* 164, 157 (1988).
80. M. W. P. L. Baars, M. C. W. van Boxtel, C. W. M. Bastiaansen, D. J. Broer, S. H. Sontjens, and E. W. Meijer, *Advanced Materials* 12, 715 (2000).
81. T. Imae, in "Structure-Performance Relationships in Surfactants: Second Edition, Revised and Expanded" (K. Esumi, Ed.). Marcel Dekker, New York, 525, 2002.
82. J. M. J. Fréchet, *Science* 263, 1710 (1994).
83. T. M. Chapman, G. L. Hillyer, E. J. Mahan, and K. A. Shaffer, *J. Am. Chem. Soc.* 116, 11195 (1994).
84. J. C. M. van Hest, D. A. P. Delnoye, M. W. P. L. Baars, M. H. P. van Genderen, and E. W. Meijer, *Science* 268, 1592 (1995).
85. J. C. M. van Hest, M. W. P. L. Baars, C. Elissen-Román, M. H. P. van Genderen, and E. W. Meijer, *Macromolecules* 28, 6689 (1995).
86. K. Aoi, A. Motoda, M. Okada, and T. Imae, *Macromol. Rapid Commun.* 18, 945 (1997).
87. J. Iyer, K. Fleming, and P. T. Hammond, *Macromolecules* 31, 8757 (1998).
88. D. Yu, N. Vladimirov, and J. M. J. Fréchet, *Macromolecules* 32, 5186 (1999).
89. C. Román, H. R. Fischer, and M. Meijer, *Macromolecules* 32, 5525 (1999).
90. J. P. Kampf, C. W. Frank, E. E. Malmström, and C. J. Hawker, *Langmuir* 15, 227 (1999).
91. K. Aoi, A. Motoda, M. Ohno, K. Tsutsumiuchi, M. Okada, and T. Imae, *Polymer J.* 31, 1071 (1999).
92. K. Aoi, K. Itoh, and M. Okada, *Macromolecules* 28, 5391 (1995).
93. K. Aoi, K. Tsutsumiuchi, E. Aoki, and M. Okada, *Macromolecules* 29, 4456 (1996).
94. M. C. Coen, K. Lorentz, J. Kressler, H. Frey, and R. Mülhaupt, *Macromolecules* 29, 8069 (1996).
95. S. Stevelmans, J. C. M. van Hest, J. F. G. A. Jansen, D. A. F. J. van Boxtel, E. M. M. de Brabander-van der Berg, and E. W. Meijer, *J. Am. Chem. Soc.* 118, 7398 (1996).

96. A. P. H. J. Schenning, C. Elissen-Román, J.-W. Weener, M. W. P. L. Baars, S. J. van der Gaast, and E. W. Meijer, *J. Am. Chem. Soc.* 120, 8199 (1998).
97. C. J. Hawker, K. L. Wooley, and J. M. J. Fréchet, *J. Chem. Soc. Perkin Trans.* 1, 1287 (1993).
98. K. Aoi, K. Itoh, and M. Okada, *Macromolecules* 30, 8072 (1997).
99. K. Aoi, H. Noda, K. Tsutsumiuchi, and M. Okada, *IUPAC 37th International Symposium on Macromolecules* 765 (1998).
100. T. Imae, K. Funayama, K. Aoi, K. Tsutsumiuchi, and M. Okada, in "Yamada Conference L, Polyelectrolytes" (I. Noda and E. Kokufuta, Eds.), 439 (1999).
101. T. Imae, M. Ito, K. Aoi, K. Tsutsumiuchi, H. Noda, and M. Okada, *Coll. Surf. A: Phys. Eng. Asp.* 175, 225 (2000).
102. M. Ito, T. Imae, K. Aoi, K. Tsutsumiuchi, H. Noda, and M. Okada, *Langmuir* 18, 9757 (2002).
103. S. Watanabe and S. L. Regen, *J. Am. Chem. Soc.* 116, 8855 (1994).
104. S. S. Sheiko, G. Eckert, G. Ignat'eva, A. M. Muzafarov, J. Spickermann, H. J. Räder, and M. Möller, *Macromol. Rapid Commun.* 17, 283 (1996).
105. S. S. Sheiko, A. M. Muzafarov, R. G. Winkler, E. V. Getmanova, G. Echert, and P. Reineker, *Langmuir* 13, 4172 (1997).
106. M. C. Coen, K. Lorenz, J. Kressler, H. Frey, and R. Mülhaupt, *Macromolecules* 29, 8069 (1996).
107. G. Bar, S. Rubin, R. W. Cutts, T. N. Taylor, and T. A. Zawodzinski, *Langmuir* 12, 1172 (1996).
108. K. Takada, D. J. Díaz, H. D. Abruña, I. Cuadrado, C. Casado, B. Alonso, M. Morán, and J. Losada, *J. Am. Chem. Soc.* 119, 10763 (1997).
109. C. B. Gorman, R. L. Miller, K.-Y. Chen, A. R. Bishop, R. T. Haasch, and R. G. Nuzzo, *Langmuir* 14, 3312 (1998).
110. D. J. Díaz, G. D. Storrier, S. Bernhard, K. Takeda, and H. D. Abruña, *Langmuir* 15, 7351 (1999).
111. R. C. Sabapathy and R. M. Crooks, *Langmuir* 16, 1777 (2000).
112. S. Loi, U.-M. Wiesler, H.-J. Butt, and K. Müllen, *Macromolecules* 34, 3661 (2001).
113. A. Sidorenko, X. W. Zhai, S. Peleshanko, A. Greco, V. V. Shevchenko, and V. V. Tsukruk, *Langmuir* 17, 5924 (2001).
114. M. Sato, J. Okamura, A. Ikeda, and S. Shinkai, *Langmuir* 17, 1807 (2000).
115. P. Wu, Q. Fan, G. Deng, Q. Zeng, C. Wang, and C. Bai, *Langmuir* 18, 4342 (2002).
116. Z. Xiao, C. Cai, A. Mayeux, and A. Milenkovic, *Langmuir* 18, 7728 (2002).
117. M. Wells and R. M. Crooks, *J. Am. Chem. Soc.* 118, 3988 (1996).
118. H. C. Yoon, M.-Y. Hong, and H.-S. Kim, *Langmuir* 17, 1234 (2001).
119. H. Zhang, P. C. M. Grim, D. Liu, T. Vosch, S. De Feyter, U.-M. Wiesler, A. J. Berresheim, K. Müllen, C. Van Haesendonck, N. Vandamme, and F. C. De Schryver, *Langmuir* 18, 1801 (2002).
120. C. A. Fail, S. A. Evenson, L. J. Ward, W. C. E. Schofield, and J. P. S. Badyal, *Langmuir* 18, 264 (2002).
121. H. Nagaoka and T. Imae, *Trans. Mater. Res. Soc. Japan* 26, 945 (2001).
122. J. Li, L. T. Piehler, D. Qin, J. R. Baker, Jr., and D. A. Tomalia, *Langmuir* 16, 5613 (2000).
123. H. Nagaoka and T. Imae, *Int. J. Nonlinear Sci. Numer. Simu.* 3, 223 (2002).
124. H. Nagaoka and T. Imae, *J. Coll. Interf. Sci.*, 264, 335 (2003).
125. K. Takeda, G. D. Storrier, M. Morán, and H. D. Abrña, *Langmuir* 15, 7333 (1999).
126. R. C. van Duijvenbode, G. J. M. Koper, and M. R. Böhmer, *Langmuir* 16, 7713 (2000).
127. R. C. van Duijvenbode, I. B. Rietveld, and G. J. M. Koper, *Langmuir* 16, 7720 (2000).
128. K. M. A. Rahman, C. J. Durning, N. J. Turro, and D. A. Tomalia, *Langmuir* 16, 10154 (2000).
129. Z. Bo, L. Zhang, B. Zhao, X. Zhang, J. Shen, S. Höppener, L. Chi, and H. Fuchs, *Chem. Lett.* 1197 (1998).
130. L. Zhang, F. Huo, Z. Wang, L. Wu, X. Zhang, S. Höppener, L. Chi, H. Fuchs, J. Zhao, L. Niu, and S. Dong, *Langmuir* 16, 3813 (2000).
131. L. Zhang, Z. Bo, B. Zhao, Y. Wu, X. Zhang, and J. Shen, *Thin Solid Films* 327–329, 221 (1998).
132. H. Tokuhisa and R. M. Crooks, *Langmuir* 13, 5608 (1997).
133. M. Zhao, H. Tokuhisa, and R. M. Crooks, *Angew. Chem. Int. Ed. Engl.* 36, 2596 (1997).
134. W. M. Lackowski, J. K. Campbell, G. Edwards, V. Chechik, and R. M. Crooks, *Langmuir* 15, 7632 (1999).
135. H. Tokuhisa, M. Zhao, L. A. Baker, Vy T. Phan, D. L. Dermody, M. E. Garcia, R. F. Feez, R. M. Crooks, and T. M. Mayer, *J. Am. Chem. Soc.* 120, 4492 (1998).
136. S.-K. Oh, L. A. Baker, and R. M. Crooks, *Langmuir* 18, 6987 (2002).
137. A. Friggeri, H. Schönherr, H.-J. van Manen, B.-H. Huisman, G. J. Vancso, J. Huskens, F. C. J. M. van Veggel, and D. N. Reinhoudt, *Langmuir* 16, 7757 (2000).
138. V. V. Tsukruk, F. Rinderspacer, and V. N. Bliznyuk, *Langmuir* 13, 2171 (1997).
139. T. Imae and N. Yoshida, unpublished data.
140. J. Wang, J. Chen, X. Jia, W. Cao, and M. Li, *Chem. Commun.* 511 (2000).
141. A. J. Khopade and F. Caruso, *Langmuir* 18, 7669 (2002).
142. A. Manna, T. Imae, M. Iida, and N. Hisamatsu, *Langmuir* 17, 6000 (2001).
143. A. Mayer and M. Antonietti, *Coll. Polym. Sci.* 276, 769 (1998).
144. L. M. Bronstein, S. N. Sidorov, P. M. Valetsky, J. Hartmann, H. Cölfen, and M. Antonietti, *Langmuir* 15, 6256 (1999).
145. N. Yanagihara, K. Uchida, M. Wakabayashi, Y. Uetake, and T. Hara, *Langmuir* 15, 3038 (1999).
146. K. Esumi, T. Hosoy, A. Suzuki, and K. Torigoe, *J. Coll. Interf. Sci.* 229, 303 (2000).
147. K. Esumi, R. Nakamura, A. Suzuki, and K. Torigoe, *Langmuir* 16, 7842 (2000).
148. K. Esumi, A. Kameo, A. Suzuki, and K. Torigoe, *Coll. Surf. A: Physicochem. Eng. Aspects* 189, 155 (2001).
149. F. Gröhn, B. J. Bauer, and E. J. Amis, *Macromolecules* 34, 6701 (2001).
150. Y.-S. Seo, K.-S. Kim, K. Shin, H. White, M. Rafailovich, J. Sokolov, B. Lin, H. J. Kim, C. Zhang, and L. Balogh, *Langmuir* 18, 5927 (2002).
151. M. Zhao, L. Sun, and R. M. Crooks, *J. Am. Chem. Soc.* 120, 4877 (1998).
152. L. Balogh and D. A. Tomalia, *J. Am. Chem. Soc.* 120, 7355 (1998).
153. K. Esumi, A. Suzuki, N. Aihara, K. Usui, and K. Torigoe, *Langmuir* 14, 3157 (1998).
154. K. Esumi, T. Hosoya, A. Suzuki, and K. Torigoe, *Langmuir* 16, 2978 (2000).
155. M. E. Garcia, L. A. Baker, and R. M. Crooks, *Anal. Chem.* 71, 256 (1999).
156. V. Chechik and R. M. Crooks, *Langmuir* 15, 6364 (1999).
157. K. Esumi, A. Suzuki, A. Yamahira, and K. Torigoe, *Langmuir* 16, 2604 (2000).
158. A. Manna, T. Imae, K. Aoi, M. Okada, and T. Yogo, *Chem. Mater.* 13, 1674 (2001).
159. F. Gröhn, B. J. Bauer, V. A. Akpalu, C. L. Jackson, and E. J. Amis, *Macromolecules* 33, 6042 (2000).
160. F. Gröhn, G. Kim, B. J. Bauer, and E. J. Amis, *Macromolecules* 34, 2179 (2001).
161. R. M. Crooks, M. Zhao, L. Sun, V. Chechic, and L. K. Yeung, *Accounts Chem. Res.* 34, 181 (2001).
162. M. F. Ottaviani, R. Valluzzi, and L. Balogh, *Macromolecules* 35, 5105 (2002).

163. A. Manna, T. Imae, K. Aoi, and M. Okazaki, *Molecular Simulation*, 29, 661 (2003).
164. K. Esumi and M. Goino, *Langmuir* 14, 4466 (1998).
165. K. Esumi, N. Fujimoto, and K. Torigoe, *Langmuir* 15, 4613 (1999).
166. K. Esumi, K. Sakagami, S. Kuniyasu, Y. Nagata, K. Sakai, and K. Torigoe, *Langmuir* 16, 10264 (2000).
167. K. Naka, Y. Tanaka, Y. Chujo, and Y. Ito, *Chem. Commun.* 1999, 1931
168. L. H. Hanus, K. Sooklal, C. J. Murphy, and H. J. Ploehn, *Langmuir* 16, 2621 (2000).
169. M. Liu, K. Kono, and J. M. J. Fréchet, *J. Controlled Release* 65, 121 (2000).
170. I. Gitsov and C. Zhu, *Macromolecules* 35, 8418 (2002).
171. P. R. Dvornic, J. Li, A. M. dė Leuze-Jallouli, S. D. Reeves, and M. J. Owen, *Macromolecules* 35, 9323 (2002).
172. M. Schlupp, T. Weil, A. J. Berresheim, U. M. Wiesler, J. Bargon, and K. Müllen, *Angew. Chem. Int. Ed.* 40, 4011 (2001).
173. D. L. Richter-Egger, A. Tesfai, and S. A. Tucker, *Anal. Chem.* 73, 5743 (2001).
174. S. Ghosh and A. K. Banthia, *Tetrahedron Lett.* 43, 6457 (2002).
175. D. Arrington, M. Curry, and S. C. Street, *Langmuir* 18, 7788 (2002).
176. F. Gröhn, X. Gu, H. Grüll, J. C. Meredith, G. Nisato, B. J. Bauer, A. Karim, and E. J. Amis, *Macromolecules* 35, 4852 (2002).
177. X. C. Wu, A. M. Bittner, and K. Kern, *Langmuir* 18, 4984 (2002).
178. J. Won, K. J. Ihn, and Y. S. Kang, *Langmuir* 18, 8246 (2002).
179. N. Feeder, J. Geng, P. G. Goh, B. F. G. Johnson, C. M. Martin, D. S. Shephard, and W. Zhou, *Angew. Chem. Int. Ed.* 39, 1661 (2000).
180. Z. Xu and W. T. Ford, *Macromolecules* 35, 7662 (2002).